

Spring 2011

Design of a bioinformatics system for insertional mutagenesis analysis and its application to the Sleeping Beauty transposon system

Kishore Nannapaneni
University of Iowa

Copyright 2011 Kishore Nannapaneni

This dissertation is available at Iowa Research Online: <https://ir.uiowa.edu/etd/1039>

Recommended Citation

Nannapaneni, Kishore. "Design of a bioinformatics system for insertional mutagenesis analysis and its application to the Sleeping Beauty transposon system." PhD (Doctor of Philosophy) thesis, University of Iowa, 2011.
<https://doi.org/10.17077/etd.y1jxbwl>

Follow this and additional works at: <https://ir.uiowa.edu/etd>

Part of the [Biomedical Engineering and Bioengineering Commons](#)

DESIGN OF A BIOINFORMATICS SYSTEM FOR INSERTIONAL MUTAGENESIS
ANALYSIS AND ITS APPLICATION TO THE SLEEPING BEAUTY TRANSPOSON
SYSTEM

by
Kishore Nannapaneni

An Abstract

Of a thesis submitted in partial fulfillment
of the requirements for the Doctor of
Philosophy degree in Biomedical Engineering
in the Graduate College of
The University of Iowa

May 2011

Thesis Supervisor: Associate Professor Todd E. Scheetz

ABSTRACT

Cancer is one of the leading causes of death in the world. Approximately one fifth of deaths in the western industrial nations are caused by cancer. Every year several hundreds of thousands of new patients are diagnosed with cancer and several thousands die of cancer. Scientists have been conducting research from different angles for effective prevention, diagnosis and cure of Cancer.

Ever since the genetic basis of cancer has been demonstrated, a race has been ignited globally in the scientific community to identify potential oncogenes and tumor suppressor genes. The genetics of the tumors are complex in nature where combinations of loss of function mutations in tumor suppressor genes and gain of function mutations in oncogenes cause cancers. The identification of these genes is extremely important to devise effective therapies to treat cancer. Insertional mutagenesis systems such as sleeping beauty provide an elegant way to identify genes involved in cancers. More and more researchers are adopting the Sleeping Beauty system for their insertional mutagenesis experiments to identify potential cancer causing genes. Given next generation sequence technologies and the vast amount of data they generate requires novel bioinformatics techniques to process, analyze and meaningfully interpret the data. The goal of this project is to develop a publicly available system for researchers worldwide to analyze the sequence data resulting from insertional mutagenesis experiments.

This system will identify and annotate all the insertion sites resulting from the sequencing of the experiment. It will also identify the Common Insertion sites (CIS) and genes with Common Insertion Sites (gCIS). The Common Insertion Sites being the

regions in the genome that are targeted more often than by chance. The whole system is accessible as a web application for use by researchers worldwide performing insertional mutagenesis experiments.

Abstract Approved: _____
Thesis Supervisor

Title and Department

Date

DESIGN OF A BIOINFORMATICS SYSTEM FOR INSERTIONAL MUTAGENESIS
ANALYSIS AND ITS APPLICATION TO THE SLEEPING BEAUTY TRANSPOSON
SYSTEM

by
Kishore Nannapaneni

A thesis submitted in partial fulfillment
of the requirements for the Doctor of
Philosophy degree in Biomedical Engineering
in the Graduate College of
The University of Iowa

May 2011

Thesis Supervisor: Associate Professor Todd E. Scheetz

Copyright by
KISHORE NANNAPANENI
2011
All Rights Reserved

Graduate College
The University of Iowa
Iowa City, Iowa

CERTIFICATE OF APPROVAL

PH.D THESIS

This is to certify that the Ph.D. thesis of

Kishore Nannapaneni

has been approved by the Examining Committee
for the thesis requirement for the Doctor of Philosophy
degree in Biomedical Engineering at the May 2011 graduation.

Thesis Committee:

Todd E. Scheetz, Thesis Supervisor

Thomas L. Casavant

Terry A. Braun

Adam J. Dupuy

Paul B. McCray

ABSTRACT

Cancer is one of the leading causes of death in the world. Approximately one fifth of deaths in the western industrial nations are caused by cancer. Every year several hundreds of thousands of new patients are diagnosed with cancer and several thousands die of cancer. Scientists have been conducting research from different angles for effective prevention, diagnosis and cure of Cancer.

Ever since the genetic basis of cancer has been demonstrated, a race has been ignited globally in the scientific community to identify potential oncogenes and tumor suppressor genes. The genetics of the tumors are complex in nature where combinations of loss of function mutations in tumor suppressor genes and gain of function mutations in oncogenes cause cancers. The identification of these genes is extremely important to devise effective therapies to treat cancer. Insertional mutagenesis systems such as sleeping beauty provide an elegant way to identify genes involved in cancers. More and more researchers are adopting the Sleeping Beauty system for their insertional mutagenesis experiments to identify potential cancer causing genes. Given next generation sequence technologies and the vast amount of data they generate requires novel bioinformatics techniques to process, analyze and meaningfully interpret the data. The goal of this project is to develop a publicly available system for researchers worldwide to analyze the sequence data resulting from insertional mutagenesis experiments.

This system will identify and annotate all the insertion sites resulting from the sequencing of the experiment. It will also identify the Common Insertion sites (CIS) and genes with Common Insertion Sites (gCIS). The Common Insertion Sites being the

regions in the genome that are targeted more often than by chance. The whole system is accessible as a web application for use by researchers worldwide performing insertional mutagenesis experiments.

TABLE OF CONTENTS

LIST OF TABLES	vi
LIST OF FIGURES	vii
CHAPTER 1 INTRODUCTION.....	1
CHAPTER 2 BACKGROUND.....	3
Cancer and its complexity	3
Cancer development.....	3
Classification of cancer-associated genes	5
Complexity of cancer	6
Current research in cancer genetics.....	7
Experimental models of cancer	8
Sleeping Beauty mediated mutagenesis	11
Analysis of insertional mutagenesis experiments	14
Specificity	14
Local hopping	14
Clonality.....	15
Common Insertion Sites (CISs)	15
gene centric Common Insertion Sites(gCIS):	16
Need for sequencing depth.....	16
CHAPTER 3 APPROACH	17
System design.....	17
CHAPTER 4 METHODS	19
Input data.....	19
Sequence analysis.....	21
Annotation.....	24
Donor chromosomes	25
Clonality.....	26
Common Insertion Sites (CIS).....	27
gene centric Common Insertion Sites (gCIS).....	27
IAS Website	28
CHAPTER 5 RESULTS	29
Resulting output files of an analysis by IAS	31
Annotation file	32

Common Insertion Sites (CIS) file.....	33
gene-centric Common Insertion Sites (gCIS) file.....	33
Support for analyzing SB experiments from multiple species.....	33
Experimental results.....	33
Detailed analysis of the lymphoma dataset.....	34
Colorectal cancers.....	39
Medulloblastomas and associated metastatic spine tumors.....	40
Skin and Liver tumors.....	41
 CHAPTER 6 DISCUSSION.....	 43
Barcode design.....	43
Removing the flanking sequences of the genomic junction fragment.....	44
Local hopping.....	45
Standard annotations.....	46
Comparison of CIS identification strategies.....	47
General utility.....	47
Beyond 2 nd generations sequencing technologies.....	48
 CHAPTER 7 FUTURE WORK.....	 52
 APPENDIX.....	 56
 REFERENCES.....	 85

LIST OF TABLES

Table 1. Summary of experiments analyzed using IAS	34
Table 2. The summary of results from the analysis of Vav, Lck and CD4 models of Lymphoma at different stages of the analysis.....	35
Table 3. Comparison of different sequencing platforms based on the read length and the number of sequences they generate and the run costs.....	48
Table A1. Common Insertion Sites (CIS) resulting from the Vav model of Lymphoma in mice.....	56
Table A2. Common Insertion Sites (CIS) resulting from the Lck model of Lymphoma in mice.....	57
Table A3. Common Insertion Sites (CIS) resulting from the CD4 model of Lymphoma in mice.....	58
Table A4. gene centric Common Insertion Sites (gCIS) resulting from the Vav model of Lymphoma in mice.....	60
Table A5. gene centric Common Insertion Sites (gCIS) resulting from the Lck model of Lymphoma in mice.....	62
Table A6. gene centric Common Insertion Sites (gCIS) resulting from the CD4 model of Lymphoma in mice.....	64
Table A7. The table below illustrates the gene pair and the p-value of the significance of the interaction for the Vav model of lymphoma in mice	69
Table A8. The table below illustrates the gene pair and the p-value of the significance of the interaction for the Lck model of lymphoma in mice	69
Table A9. The table below illustrates the gene pair and the p-value of the significance of the interaction for the CD4 model of lymphoma in mice	69
Table A10. Common Insertion Sites (CIS) resulting from the Colorectal cancer dataset (Starr et al).....	70
Table A11. gene centric Common Insertion Sites (gCIS) resulting from the Colorectal cancer dataset(Starr et al)	73
Table A12. Common Insertion Sites (CIS) resulting from the Liver tumor dataset.	83
Table A13. gene centric Common Insertion Sites (gCIS) resulting from the Liver tumor dataset	83
Table A14. Common Insertion Sites (CIS) resulting from the Skin cancer dataset.....	84
Table A15. gene centric Common Insertion Sites (gCIS) resulting from the Skin cancer dataset.	84

LIST OF FIGURES

Figure 1. Structure of Sleeping Beauty Transposon System adapted from Dupuy et al	12
Figure 2. In the first two transcripts Sleeping Beauty drives the expression of the gene and in the last two transcripts it disrupts the transcript. This figure is adapted from Dupuy et al (Dupuy et al., 2006).	13
Figure 3. System diagram.....	18
Figure 4. Sample sequence file.....	19
Figure 5. Example barcode file	20
Figure 6. Sequence structure	21
Figure 7. Sequence associated with tumor 472-4T	22
Figure 8. Sequences associated with tumor 472-4T after removing the inverted repeat sequence and the adaptor sequence	23
Figure 9. The annotation of genomic junction fragments from Figure 8	25
Figure 10. IAS login Page	29
Figure 11. IAS page where the title of the Experiment, the host organism and the barcode and the sequence file are uploaded to the IAS server.....	30
Figure 12. Screen shot of the listing of all the input and the results on the My Integrations page on the IAS website.....	32
Figure 13. Pathway observed in Vav models of Lymphomas in mice.....	36
Figure 14. Pathway observed in Lck models of Lymphomas in mice	37
Figure 15. Pathway observed in CD4 models of Lymphomas in mice.....	40
Figure 16. The extent of overlap between CIS. gCIS identified by IAS and CIS's identified by method specified in Starr et al	41

CHAPTER 1

INTRODUCTION

Insertional mutagenesis has been increasingly being used as a platform to identify potential disease causing genes. Researchers use insertional mutagens such as retroviruses and transposable elements to cause mutations. An essential feature of insertional mutagenesis, is that the inserted elements provide sufficient unique sequence to allow them to be molecularly isolated – allowing identification of the affected loci (Collier, Carlson, Ravimohan, Dupuy, & Largaespada, 2005). Biospecimens are selected based upon phenotype, and the genomic locus of the insertion is extracted and sequenced. Such experiments provide an association between the selected phenotype and the locus/gene at which the insertion occurred. Insertional mutagenesis is increasingly popular in the cancer research community, in which researchers are using them for forward genetic screens to identify cancer-causing genes (Dupuy, Jenkins, & Copeland, 2006).

The Sleeping Beauty transposon system is one such platform for insertional mutagenesis, and is the foundation upon which this thesis was developed. Sleeping Beauty can be activated in a tissue specific manner in the somatic cells of the host organism (Dupuy et al., 2006). Tumors are harvested, from which genomic DNA is extracted and sequenced. Insertional mutagenesis experiments typically result in hundreds of thousands to millions of sequences, and therefore require efficient computational techniques for their analysis. With the advances in next generation sequencing technologies the number of reads per run is expected to reach billions in the future.

Investigators want to know the location of these integrations in the host genome. Integrations required for tumor development and progression (driver mutations) will be clonally selected throughout all of the cells in the tumor (Vrieze et al, In preparation).

However, random integrations (passenger mutations) will also be frequently observed, as these are independently accumulating in the cells. Thus thousands of integrations may be observed from each tumor, requiring differentiation between the (causative) driver mutations and the (random) passenger mutations.

The scientific community using transposon-based insertional mutagenesis screens to identify cancer-causing genes is growing and is expected to continue to grow. The Sleeping Beauty system is especially appealing given its various advantages over retroviruses and other transposons, which are described in detail in the “Background” chapter of this dissertation.

Given the rising number of researchers using the Sleeping Beauty system as forward genetic screens to identify cancer causing genes, and the enormous amounts of sequence data the experiments generate, necessitates the design and development of efficient computational algorithms and techniques for their analysis. Such a bioinformatic system must be able to identify the location of insertions in the host organism and subsequently identify the region(s) or gene(s) that are causally involved. The system should be available to researchers worldwide for the analysis of their insertional mutagenesis sequence data.

Integration analysis system (IAS) is a bioinformatics system that is designed, developed and made available to the research community using insertional mutagenesis to identify cancer-causing genes via a web application. IAS not only identifies the location of the integration events in the host genome but also analyzes these integration sites for potential interesting loci and genes that could play a causal role in cancer. Results of some the analyses using IAS are presented in the “Results” section, and enhancements to the design of the system given changes in the experimental design or sequencing platform are presented in the “Discussion” and “Future work” of this thesis.

CHAPTER 2

BACKGROUND

Cancer and its complexity

Cancer is a term for diseases in which abnormal cells divide without control. Cancer cells often invade nearby tissues and can spread via the bloodstream and lymphatic system to other parts of the body. Cancers are classified according to the tissue and cell type from which they arise (Schulz, 2007). The abnormal growth, invasiveness and metastasis are the primary characteristics of cancer (Hanahan & Weinberg, 2000).

Since the genetic makeup varies only moderately between individuals from different parts of the world, the varying incidences of cancer over time and geographical locations can largely be attributed to environmental factors. These exogenous factors are typically assorted into the following three classes: chemical, physical and biological carcinogens. An individual's risk of cancer also depends on an individual's tolerance to these environmental factors based on their genetic makeup. Endogenous processes such as DNA replication, chronic inflammation and metabolic processes involving the creation of reactive oxygen species can also increase the likelihood of cancer progression by acting in cooperation with the exogenous carcinogens (Schulz, 2007).

Cancer development

Mutations in either oncogenes or tumor suppressor genes are believed to be essential for cancer initiation. Oncogenes operate in a dominant fashion, where a mutation in a single copy of the gene is sufficient for cancer initiation. In contrast, tumor suppressor genes typically operate in a recessive fashion in which both the copies of the gene must be inactivated for cancer initiation (Schulz, 2007). Studies indicate that mutations in a single oncogene or tumor suppressor are insufficient to cause a cancer.

Instead, cancer initiation thought to require at least 4 or 5 successive mutations in a significantly important pathway (Pedraza-Farina, 2006).

Initiation is followed by tumor progression. Some tumors grow rapidly, and some slowly. Tumor initiation involves dysregulation of the natural processes that regulate cell growth (Pedraza-Farina, 2006). In contrast, the process of tumor progression modifies the cell and its environment to allow continued tumor growth. One such example for solid tumors is the need to increase blood-flow to the local environment, often involving the growth of new blood vessels. In addition, different tumors may have radically differing lethality. They are classified into various grades from low to high based on a set of physical markers. High-grade tumors are more malignant in nature and therefore tend to have more detrimental outcomes in terms of cancer progression. In contrast, low-grade tumors are early lesions, which may progress to more malignant and invasive high-grade tumors. Understanding the set of sequential mutations and/or disruptions of pathways that can transform a low grade tumor to a high grade tumor is extremely crucial for cancer containment and therapy (Pedraza-Farina, 2006).

Tumors often metastasize. In metastasis the cancerous cells not only grow uninhibited in the tissue of origin but also invade and proliferate to other tissues. Some normal physiological processes (e.g., wound healing) involve cell proliferation. These regulatory processes are either deactivated or lose function during invasion and metastasis (Pedraza-Farina, 2006). Several families of genes are involved in cell proliferation, including: integrins, intracellular matrix degrading enzymes, cell-cell adhesion molecules and signaling pathways. Loss of intended function of these genes or their involved pathways can lead to invasion and metastasis. Studies suggest that at least four genes in such critical pathways have to be disturbed for cancer metastasis (Pedraza-Farina, 2006).

Classification of cancer-associated genes

Genes may have differing effects within the development and progression of cancer. The first are oncogenes - these are genes that perform normal activities in the cell. In their pre-cancerous form, they are referred to as proto-oncogenes, and when mutated become oncogenes (Schulz, 2007). If a mutation is acquired by the proto-oncogene by any of the above stated carcinogens the gene may be turned on or off in a way that's harmful to the cell and causes cancer. Many oncogenes result from a dominant negative action – either through the acquisition of a new function, or through inappropriate expression. Thus, often only a single copy of the oncogene must be mutated (rather than both copies) (Schulz, 2007). Although there are known cases of inherited mutations in oncogenes, they are mostly acquired via *de novo* mutations (<http://www.cancer.org>).

The other category of cancer-associated genes is the tumor suppressor genes. These are genes that usually oversee activities like DNA repair, cell division and programmed cell death. Commonly, the functions of these genes are such that a single copy is sufficient for proper function. Thus, both copies are typically mutated in cancers (Schulz, 2007). As with the oncogenes, there are cases of inherited mutations in these genes but most are acquired (<http://www.cancer.org>).

The mutations may also be classified as “driver” or “passenger”. Driver mutations are mutations that have a causative role in cancer. These may occur in both oncogenes and tumor suppressors. In contrast, passenger mutations do not have a role in the initiation of cancer. Instead these are the mutations that occur by chance, are in the same cell(s) serving as the initial cancer progenitor. These mutations have no selective advantage, are obtained by chance, and are present through subsequent cell division and expansion (Wood et al., 2008).

Complexity of cancer

Cancer is a multi-factorial and complex condition in which multiple genetic and environmental factors jointly cause cancer. Cancers typically involves multiple aberrations in a cell's genome. These aberrations may take many forms from changes in a single nucleotide to copy number changes that alter the structure or number of one or many genes, to structural abnormalities that result in the reorganization of a region of a chromosome (inversions) or even the rearrangements of entire chromosomes (translocations). Extreme cases of cancerous cells often have increased copy number of multiple chromosomes. Most cancer-causing mutations are somatic (i.e. not found in the parents) although there can be inherited mutations which increase the risk of cancer susceptibility. Inherited mutations are rare and a person's genotype only slightly affects the initiation or progression of cancer. Other factors such as epigenetics and mutations during fetal development can also cause cancer (Schulz, 2007).

The single base changes, insertions and deletions chromosomal translocations and inversions give rise faulty proteins by either reducing the function of a tumor suppressor gene or adding functionality to the proto-oncogene. Both oncogenes and tumor suppressor genes are observed consistently in cancer cells. The varying number of chromosomes: if there multiple copies of a chromosome it over expresses some of its genes like wise if there are few or no copies of the chromosome some of genes are lost or under expressed (Schulz, 2007).

These genetic alterations occur in varying magnitudes in various types of cancers. Some cancer might have just point mutations while others may have extreme chromosomal abnormalities. The complexity of cancer is further increased by epigenetic changes that also may alter the risk of developing a tumor (Schulz, 2007).

Current research in cancer genetics

Research has been conducted from various fronts to understand the processes involved in cancer initiation and progression, and to distinguish different categories of tumors. Two primary goals underlie these efforts: to understand the cause of cancer and eventually cure/prevent it from occurring, and to better treat those patients that are already victims of cancer. Multiple, genome-wide approaches have been employed including assessment of gene expression, high-density genotyping, genome sequencing, screens for epigenetic patterns of methylation, copy number changes. As an example, expression microarrays provide a quantitative snapshot of expression on a genomic scale (Slonim & Yanai, 2009). A common strategy with this data is to utilize unsupervised learning methods (such as Class Discovery) to determine the patterns of gene expression that are associated with subclasses or a particular class of cancer. All the samples are used without any prejudiced assumptions. The unsupervised clustering algorithms generate dendrograms in which the samples are clustered in a hierarchical fashion on one axis and the genes themselves on the other axis. Such unsupervised learning can also be used to discover new classes of cancer based on the expression signature. Examples of unsupervised learning algorithms used in analysis of microarrays include Hierarchical clustering, Self Organizing maps, k-means clustering and principal component analysis (Matros, Wang, Richardson, & Iglehart, 2004).

Supervised learning is used for class prediction where the underlying algorithms identifies unique pattern of gene expression from known tissue samples (e.g. tumor, normal or metastasis or response to stimuli or drugs) and then can predict the class of the unknown tissue sample based on its expression signature. Examples of supervised learning algorithms used in the analysis of microarrays include artificial neural networks, support vector machines, k-nearest neighbors and decision trees (Matros et al., 2004).

Cancer tissues often exhibit aneuploidy – an abnormal number of chromosomes. High copy number for gene EFGR was observed in non-small cell lung cancer and is

associated to efficacy of drug gefitinib in treating those tumors (Cappuzzo et al., 2005). The most common technology used to detect copy number changes are genome-wide, high-density arrays. These work based upon hybridization intensity of locus-specific probes, such as in comparative genome hybridization (CGH). Easton et al used arrays interrogating 227876 SNP's to identify risk-associated genes in breast cancer. They have identified four potentially causal genes in this study (Easton et al., 2007). Li et al used ArrayCGH to assess the role of miRNA's in diffuse large B-cell lymphoma (DLBCL). They used Array CGH to obtain miRNA copy number data and used a permutation analysis to identify statistically significant altered miRNA's (C. Li et al., 2009). Vogelstein et al sequenced 20857 transcripts from 18,191 genes and identified genes that are mutated in 11 breast and 11 colorectal tumors. A gene that had a mutation in a tumor and not in the normal tissue is further sequenced. These genes were further analyzed vis-à-vis their involvement in pathways and protein interaction. The study concluded that there are approximately 15 genes that harbor driver mutations responsible for initiation, progression and maintenance of a tumor (Wood et al., 2008).

Experimental models of cancer

Various models have been used to understand the initiation and progression of cancer to eventually identify drugs or therapies. These include naturally occurring models (e.g., cell lines and strains/sub-species of animals) and induced models (e.g. via chemical exposure, radiation or biological vectors).

Immortalized cancer cells have long been used in molecular experimentation to understand cancer. These cell lines provide a virtually unlimited supply of cancer cells for experimentation. The principal drawback of cell lines is that they represent a subgroup of cancer classes and are often contaminated by other cell lines.

Mice have long been used as a model of human disease mainly because they are mammals (i.e. "human-like"), easy to handle and have a rapid life cycle. The high tumor

incidence and rapid tumor growth make them specially suited for cancer models. They are very well studied and characterized amongst all mammals. Mouse models have been extremely critical in understanding cancer initiation and progression. They can be used to study cancer progression by a carcinogen, and may also be used to study the effect of a therapeutic agent.

ENU, shorthand for N-ethyl-N-nitrosourea, is a very powerful mutagen, causing a loss of function mutation usually targeting the spermatogonial stem cells inducing one point mutation every 1-2Mb of the genome (Kile & Hilton, 2005). ENU is so potently mutagenic that it overcomes the cell's inherent DNA proofreading and repair mechanisms (Russell et al., 1979) Thus ENU makes a potent forward genetic screen in mice, in which mice are mutated first, and those that develop a desired phenotype are selected for follow-up. Although ENU is an efficient mutagen, the process of identifying the causative mutations requires cloning and/or mapping of the genes based upon multiple generations of backcrosses. Thus cloning the gene(s) responsible for a given phenotype is a difficult and a laborious process (Amsterdam et al., 1999).

Insertional mutagenesis is the process of mutating the genomic DNA by adding one or more bases. Insertional mutagens are usually viruses or transposable elements (transposons). These insertional mutagens integrate within the genome of the host organism, potentially disrupting (or inducing) one or more nearby genes. The host organism develops a phenotype due to a loss or gain of function mutation in its cells. The insertion events in the whole genome of the organism can be sequenced by identifying the location of transposon or a virus and associate a particular locus to the resulting phenotype.

Insertional mutagenesis can be used as a potent forward genetic screen to model cancer in organisms like mice. This may require screening many individual mice given the complexity of cancer to obtain significant results. Forward genetic screens using insertional mutagenesis can be very rewarding in understand disease. One example of an

insertional mutagen is the P-element, a transposon, commonly used in *Drosophila melanogaster* to understand the function of a gene based on the phenotype it produces when inserted (and hence deactivated) with the P-element. Similarly the Ti plasmid is used to study gene function in plants. Although insertional mutagenesis is not as potent as ENU or other chemical carcinogen the inserted sequence is sufficiently long to allow for molecular isolation, making it comparatively easy to sequence the region surrounding the insertion.

One class of commonly used insertional mutagens is viral mutagens including MuLV and MMTV. MuLV is a popular insertional mutagen in mice. New-born mice are infected with MuLV before they have developed a immune system. The viraemia spreads in the mice unabatedly mostly proliferating particularly through the cells of the immune system. The viral insertions are spread throughout the genome activating oncogenes are deactivating tumor suppressor genes causing tumors. These tumors can be retrieved and the genomic junctions fragments sequenced and thus identify the location of the insertion in the host genome. The MuLV mainly causes Hematopoietic malignancies (Kool & Berns, 2009). Jonkers et. al. have used M-MuLV insertional mutagenesis in mice to implicate *Frat1* gene to be collaborating with *Myc* and *Pim1* in Lymphomas (Jonkers, Korswagen, Acton, Breuer, & Berns, 1997).

MMTV is another popular insertional mutagen in mice and primarily causes breast tumors. Theodorou et. al. have used the MMTV to identify novel genes involved in mammary tumors. They have identified 13 new genes that have not been previously implicated in breast cancer and 17 novel genes that have never been associated with cancer (Theodorou et al., 2007).

Retroviruses have significant limitations with regards understanding cancer. They appear to be able to only induce hematopoietic and breast tumors. Most of the human cancers are solid originating in somatic cells. Also viruses appear to have hot spots for integrations targeting only particular regions in the genome due to several factors, which

include the cell type, organism and multiplicity of the infection and design of the vector (Moressi, 2007) . For example HIV prefers to integrate within active genes and MuLV has a bias towards the 5' end of the genes.

A second class of insertional mutagens are based upon transposable elements (Transposons). These are chunks of DNA that move within the genome and also between species. There are two types of transposons, retrotransposons and DNA transposons. The retrotransposons are transcribed into RNA and subsequently reverse transcribed to be integrated into the genome. The DNA transposons are ones where the DNA moves from one part of the genome to another in a cut and paste fashion with the help of transposase (Griffiths, Miller, Suzuki, Lewontin, & Gelbart, 2000). The transposon requires assistance in the form of a protein coding gene (transposase) to perform the cut-and-paste process of transposition.

Transposons contain unique sequences, which help in identifying the location of the integrations sites. This ability of the transposons to migrate within the genome and being able to identify the site of integration renders them a powerful tool in insertional mutagenesis experiments (Weaver, 1998). Some examples of transposons widely used in insertional mutagenesis experiments are the Sleeping Beauty (SB) and P-elements.

Both SB and P-elements are isolated from naturally occurring organisms. In the case of SB, substantial modifications have been incorporated to enhance its ability to cause the development of cancer.

Sleeping Beauty mediated mutagenesis

The Sleeping Beauty is a DNA transposon which migrates from one part of the genome to the other by a cut and paste mechanism. The system primarily comprises two parts - the transposon itself and a transposase to drive the transposition. The initial Sleeping Beauty system consisted of a transposase source RosaSB knock in allele and the transposon T2/Onc2. The SB is engineered to contain two splice acceptors and bi-

directional poly adenylation signals. It also contains a retroviral LTR a splice donor. The T2/Onc2 transposon with the help of transposase randomly integrates at a TA dinucleotide junction in the genome (Dupuy, Akagi, Largaespada, Copeland, & Jenkins, 2005). Since the transposons are tagged the location of the insertion in the genome can be subsequently identified thus identifying the cancer causing genes. Substantial number of mice died during embryogenesis and the surviving ones ended up having aggressive tumors. Although the system generated tumors, they were mostly hematopoietic. Most of the tumors prevalent in humans are solid tumors (Dupuy et al., 2006).

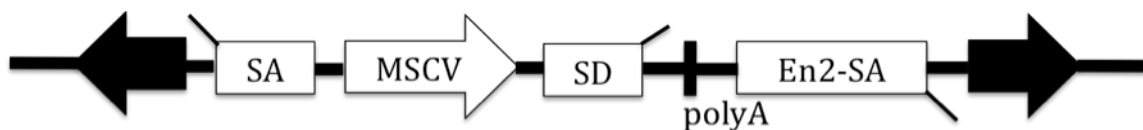


Figure 1. Structure of Sleeping Beauty Transposon System adapted from Dupuy et al

A new T2/Onc3, RosaSBLSL was designed to overcome the existing limitations of the T2/Onc2, RosaSB system. The T2/Onc2 is modified by replacing the retroviral LTR with a CAG promoter to give T2/Onc3. T2/Onc3 transposes ubiquitously as opposed to transposition only in the hematopoietic cells. The RosaSB is placed under the control of a lox-stop-lox cassette to drive its expression in a Cre dependent manner giving the capability of being expressed only in tissues of interest (Dupuy et al., 2005). Sleeping Beauty can induce insertional mutagenesis in germ line as well as somatic cells. The structure of the Sleeping Beauty transposon system is shown in Figure 1.

There are multiple ways in which the Sleeping Beauty mutagenesis can occur as shown in Figure 2. Since the transposon carries a promoter and a splice site the

transposon can drive the expression of a subsequent oncogene given it integrates upstream of the gene. If the transposon integrates within a gene it can drive the expression of the truncated oncogene. Likewise the transposon can also disrupt the expression of the gene and produce a truncated transcript when it integrates within in a gene because of the presence of the bidirectional polyadenylation signals as shown in Figure 1. These features of the Sleeping Beauty system renders it a powerful tool in identifying genes involved in cancers thus aid in identifying potential new therapies.

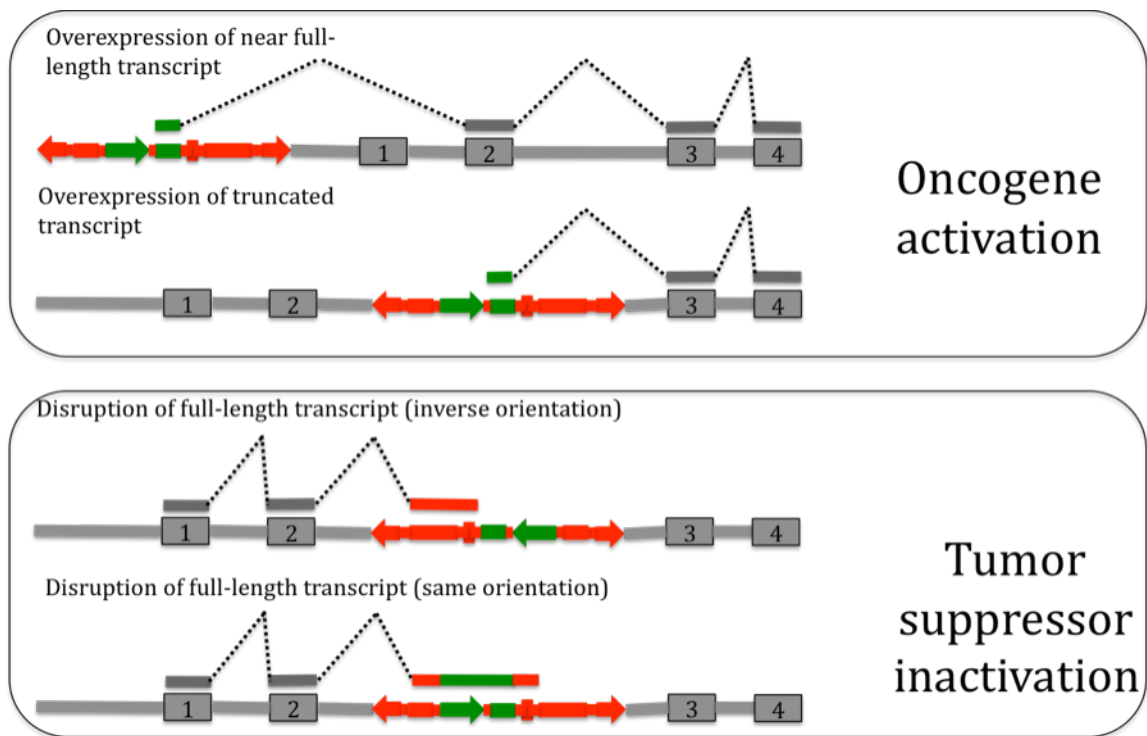


Figure 2. In the first two transcripts Sleeping Beauty drives the expression of the gene and in the last two transcripts it disrupts the transcript. This figure is adapted from Dupuy et al (Dupuy et al., 2006).

In contrast to the P-elements in *Drosophila*, Sleeping Beauty does not seem to show such affinity for hot or cold spots in the genome. Instead, Sleeping Beauty appears

to randomly integrate at a TA dinucleotide junction anywhere in the genome. Retroviruses have significant limitations with regards understanding cancer. They appear to be able to induce hematopoietic and breast tumors. Most of the human cancers are solid originating in somatic cells. Also viruses appear to have hot spots for integrations targeting only particular regions in the genome due to several factors which include the cell type, organism and multiplicity of the infection and design of the vector (Moressi, 2007). Finally Sleeping Beauty is autonomous meaning it does not need any extracellular substances for its transposition activity.

Analysis of insertional mutagenesis experiments

The focus of this thesis is the analysis of experiments based upon the Sleeping Beauty insertional mutagenesis system. Several issues are of critical importance in the analysis of insertional mutagenesis experiments using the Sleeping Beauty system. These include specificity, local hopping of the transposon, identification of the clonally expanded integration sites and determination of loci at which integrations commonly occur. These issues are described below.

Specificity

The SB junctions are retrieved using LM-PCR and are sequenced. The location of the genomic junction fragment thus obtained needs to be ascertained. The retrieved genomic junction fragments have to be of sufficient length in order to be unambiguously aligned to the genome.

Local hopping

In general, SB transposase allows SB transposons to be excised and re-integrated at a random position. However, a small fraction of the re-integrations occur locally (within 20 Mb of the site of excision). This yields a biased integration pattern in which loci near the donor cassette have an increased likelihood of SB integration, leading to a

different prior probability of integration than the rest of the genome. This phenomenon is termed as Local Hopping and can contribute to the identification of insertions that are false positives.

Clonality

While insertions that were repeatedly identified across tumors are probably driver mutations, the insertions that are identified infrequently are more likely to be passenger mutations caused by the continued transposition events not positively selected in tumorigenesis. An estimate for the extent of clonality needs to be developed to eliminate the background transposition events and identify driver mutations.

Common Insertion Sites (CISs)

Most of the SB screens generate thousands of insertions. For example Starr et al have recovered approximately 17000 insertion sites from a SB screen of colorectal cancers (Starr et al., 2009). While a few insertions legitimately cause cancer other are probably acquired by continued SB insertions. These passenger mutations are usually dormant and have no effect in tumor initiation and development. It is important to identify the genes or regions that are positively selected for tumor initiation, development and metastasis. Distinguishing these driver mutations from passenger mutations is necessary in devising subsequent therapies. Common insertions sites are the regions in the genome that repeatedly harbor insertions across multiple tumors at higher frequencies than expected by chance. If these regions are observed to have insertions frequently across independent tumors they are more likely to be responsible for the tumor initiation and development by applying guilt by association approach.

gene centric Common Insertion Sites(gCIS):

While CIS identify regions in the genome, genes are the functional regions in the genome that serve as a blue print for proteins. Identifying the genes having insertions higher than expected by chance is a better approach towards identifying genes involved in cancer rather than computing the CIS and identify the genes in its neighborhood. The end goal of most insertional mutagenesis studies is to identify the gene involved in cancer and have a gene centric approach is more rewarding than the traditional approach of identifying the CISs.

Need for sequencing depth

Identifying a few insertions per tumor will reduce the capabilities to identify CIS, gCISs and genes cooperating in cancer accurately. More the number of insertions sequenced and aligned to the host genome per tumor better is the statistical power.

The sequencing depth is essential for identifying genes cooperating in tumorigenesis. Since the CISs and gCISs are defined as loci in the genome that have more insertions than expected the number of tumors sequenced is important for identifying CISs and gCISs. It is important to sequence adequate number of tumors as well as adequate number of insertions per tumor to effectively identify CISs, gCISs and cooperating genes. All these issues have to be taken into consideration before the design of an insertional mutagenesis experiment.

CHAPTER 3

APPROACH

The primary focus of this thesis is the development of an analysis pipeline for insertional mutagenesis experiments using the Sleeping Beauty transposon system or simply the SB system. The analysis pipeline is the computational engine behind IAS – the Integration Analysis System. The acronyms SB and IAS are used throughout this document interchangeably for Sleeping Beauty and Integration Analysis System. This chapter describes the strategy developed to analyze the genomic fragments adjoining SB integration events. This section also explains the algorithms developed, techniques used and the methods adopted to evaluate everything from identifying the location of the inserts in the genome to identifying the CISs and gCISs.

System design

A system diagram of the analysis pipeline is shown in Figure 3. The system requires two files as inputs: a multi-sequence FASTA file, and a barcode file containing the analysis parameters. The barcode file is needed, because a standard next-generation sequencing experiment provide sequences enough to characterize many tumors. The tumor-specific metadata required to accurately process the resulting pooled set of sequences is contained in the barcode file.

Using the parameters from the barcode file, the system classifies the sequences from the sequences files into individual tumor files. The sequences flanking each genomic junction fragment are identified, and the genomic junction fragment is isolated. These genomic sequences are aligned to the genome of the host organism, providing the set of integration sites. These integration sites are subsequently annotated and the regions and genes that are statistically over-represented are identified.

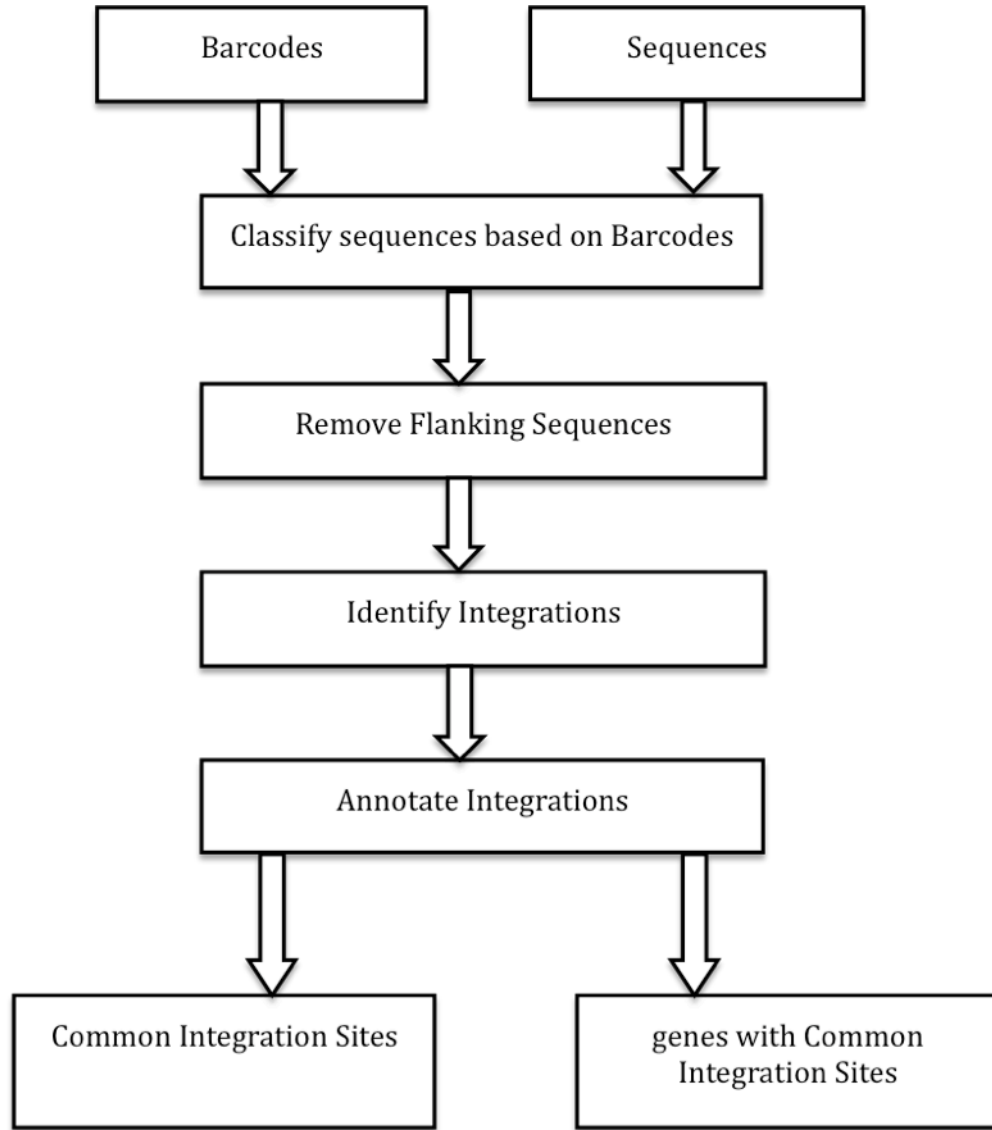


Figure 3. System diagram

CHAPTER 4

METHODS

Input data

The sequences generated from a SB insertional mutagenesis experiment with the specification of certain parameters are primary inputs to the IAS system. The IAS system requires two files as input. The first file contains the sequences, and the second contains the per-tumor metadata required for analysis.

The sequence file is a multiple-sequence FASTA format file containing the sequences from a SB mutagenesis experiment. Figure 4, below, provides a listing of several FASTA-formatted sequences. Sequence files typically contain hundreds of thousands to millions of sequences. Each sequence is represented by a header line, in which a leading ‘>’ (greater than symbol) is followed by the sequence name and (optionally) descriptive information is presented. In Figure 4, a partial sequence file is presented with descriptive data from a Roche/454 sequencing experiment.

```
>FZMARUM01ASN6F rank=0490328 x=209.0 y=1749.0 length=97
CAAGACTGTCGACTCCAACCTAAGTGTATGTAACTTCCGACTTCAACTGTATGTACCGTTCTGAAGTCTCCAACCTAGTCCCTTAAGC
GGAGCCCT
>FZMARUM01B5PB5 rank=0010687 x=767.0 y=3827.0 length=89
GAAGTGCCTCCGACTCCAACCTAAGTGTATGTAACTTCCGACTTCAACTGTATAAAGCAAATCCATACCTAGTCCCTTAAGCGGAGCCC
>FZMARUM01CL4BT rank=0431354 x=954.0 y=3799.0 length=101
CAAGACTGTCGACTCCAACCTAAGTGTATGTAACTTCCGACTTCAACTGTACATGGCACTGTACCTCATTATCTGACACTAGTCCCTT
AAGCGGAGCCCT
>FZMARUM01D17W9 rank=0010731 x=1548.0 y=1547.0 length=86
GAAGTGCCTCCGACTCCAACCTAAGTGTATGTAACTTCCGACTTCAACTGTAAATTAGCCTGTACCTAGTCCCTTAAGCGGAGCCC
>FZMARUM01AU68Z rank=0432580 x=238.0 y=993.0 length=106
CAAGACTGTCGACTCCAACCTAAGTGTATGTAACTTCCGACTTCAACTGTATGTACTTGTAAATAGACACAAATGAATCAATGCCTAGT
CCCTTAAGCGGAGCCCT
```

Figure 4. Sample sequence file

The barcode file contains the tumor-specific metadata required for the accurate analysis of the sequences. The barcode file is provided as an Excel-compatible, tab-delimited text file. Each row of the file represents a unique combination of tumor and IRR/IRL. For each barcoded sample, this files contains:

- * oligonucleotide barcode,
- * tumor ID,
- * orientation of the cloning sequence (IRR/IRL),
- * flanking sequences (SB inverted repeat and 3' adaptor), and
- * the donor chromosome (location of the SB cassette).

The barcode sequence is used to uniquely associate each sequence with a tumor. The flanking sequences describe the specific sequences that all SB insertion derived sequences should contain – both an SB subsequence in front and an adaptor sequence after. These sequences are used to identify and remove the non-genomic portions of the experimental sequences. The donor chromosome specifies, for that particular tumor, the chromosome within which the SB cassette is located. This is critical in removing background integrations present due to the “local hopping” process of SB. Removal of these “local hops” is needed for the accurate identification of common integration sites. A sample barcode file is shown in Figure 5. As shown in Figure 3, the barcode file and the sequence file are the primary inputs to the system.

```
CAAGACTGTC 472-4T IRL GACTCCAACCTTAAGTGTATGTAAACTTCCGACTTCAACTG GTCCCTTAAGCGGAGCCC chr4
GAAGTGCTCC 3437-1T IRL GACTCCAACCTTAAGTGTATGTAAACTTCCGACTTCAACTG GTCCCTTAAGCGGAGCCC chr4
AGTCCAATCG 472-3T IRL GACTCCAACCTTAAGTGTATGTAAACTTCCGACTTCAACTG GTCCCTTAAGCGGAGCCC chr4
GAGCCTGACT 471-1T IRL GACTCCAACCTTAAGTGTATGTAAACTTCCGACTTCAACTG GTCCCTTAAGCGGAGCCC chr4
```

Figure 5. Example barcode file.

This shows a sample barcode file providing the metadata for four tumors: 472-4T, 3437-1T, 472-3T and 471-1T. As expected, for an analysis based upon a single

experiment, all of the adaptor sequences are identical, as is the flanking sequence from the IR portion of the SB element.

The structure of the experimental sequences from SB-derived tumors is shown in Figure 6.



Figure 6. Sequence structure

The first part of the sequence in Figure 6 is a barcode, which uniquely associates a sequence to a particular tumor. IRL/IRR is a partial sequence from the left or right inverted repeat of the transposon, based on its orientation. The genomic sequence is the genomic junction of the host organism that is adjacent to the SB integration. The sequences may be followed by an adaptor sequence, depending on the length of the sequence and the length of the genomic fragment.

Sequence analysis

As shown in Figure 8, the sequence structure has four parts, the first part being the barcode. The barcode is typically a 6-12 nt oligonucleotide sequence at the beginning of each read in the sequence. This allows next generation sequencing runs to be performed using pools of tumors simultaneously, while still enabling the unique association of each sequence with a specific tumor. The barcode-based tumor identification process splits the input sequence file into per-tumor FASTA files. The barcode comparison utilizes the first N nts of every sequence in the input sequence file to the set of per-tumor barcodes, where N is the length of the barcodes utilized in the pooled tumors. The comparison is performed using the Levenshtein distance metric, often

referred to as the edit distance (Levenshtein,). The Levenshtein distance metric is a more robust metric than the Hamming distance, as it allows for both nucleotide mis-matches and insertions/deletions. If the Levenshtein's distance between the first N nts and a given barcode is less than two, the sequence is classified as the tumor associated with that barcode and included in the per-tumor file with the barcode removed from the sequence. The sample barcode file in Figure 5, utilizes 10 nt barcode. The sequences in Figure 4 with the first 10 base pairs highlighted in red are mapped uniquely to the tumor identified as 472-4T and the sequences with the first 10 base pairs highlighted in green to the tumor identified as 3437-1T. Such uniquely associated sequences with tumors are transferred to per-tumor fasta file after removing the barcodes from the sequences. These files are named after the tumor. Several sequences associated with tumor 474-4T are shown in Figure 7.

```
>FZMARUM01ASN6F rank=0490328 x=209.0 y=1749.0 length=97
GACTCCAACCTAAGTGTATGTAAACTCCGACTTCAACTGTATGTCACCGTTCTGAAGTCTCCAACCTAGTCCCTTAAGCGGAGCCCT
>FZMARUM01CL4BT rank=0431354 x=954.0 y=3799.0 length=101
GACTCCAACCTAAGTGTATGTAAACTCCGACTTCAACTGTACATGGCACTGTACCTCATTATCTGACACTAGTCCCTTAAGCGGAGCC
CT
>FZMARUM01AU68Z rank=0432580 x=238.0 y=993.0 length=106
GACTCCAACCTAAGTGTATGTAAACTCCGACTTCAACTGTATGTACTTGTAATAGACACAAATGAATCAATGCCTAGTCCCTTAAGCG
GAGCCCT
```

Figure 7. Sequences associated with tumor 472-4T

The flanking sequence removal process trims the adaptor and the partial inverted repeat sequence specified in the barcodes file from each experimental sequence, to ensure accurate integration site mapping. `cross_match` is used to remove the partial sequences derived from the SB element and the adaptor sequence. A mismatch rate of ten percent is used to allow for the presence of sequencing errors in the sequences. Given a set of reads and flanking sequences `cross_match` removes the flanking sequences

from the reads leaving an unadulterated set of genomic junction fragments. The `cross_match` program is used to align a nucleotide sequence or sequences against a database of sequences (Gordon, 2003) (Ewing & Green, 1998). Primarily designed to identify vector sequences in a set of reads. This can be used to removed the IRL/IRR and the Adaptor sequences from the reads obtained by transposon based insertional mutagenesis screens. At this point the tumor files have just the genomic DNA in them as shown in Figure 8. The inverted repeat sequence highlighted in yellow and adaptor sequence highlighted in blue in Figure 7 for tumor 472-4T are removed using `cross_match` and the remaining genomic junction fragment is presented in Figure 8.

```
>FZMARUM01ASN6F rank=0490328 x=209.0 y=1749.0 length=97
TATGTCACCGTTCTGAAGTCTCCAACATA
>FZMARUM01CL4BT rank=0431354 x=954.0 y=3799.0 length=101
TACATGGCACTGTACCTCATTATCTGACACTA
>FZMARUM01AU68Z rank=0432580 x=238.0 y=993.0 length=106
TATGTACTTGTAAATAGACACAAATGAATCAATGCCTA
```

Figure 8. Sequences associated with tumor 472-4T after removing the inverted repeat sequence and the adaptor sequence.

The classification of the sequences into individual tumor files combined with `cross_match` allows IAS to perform the analysis on a per tumor basis instead on a per sequence basis. The trimmed sequences are aligned to the host organism's reference genome using BLAT. BLAT (Blast Like Alignment Tool) is used for rapid alignment of sequences against the genome. BLAT achieves this by storing the index of the genome in the memory (Kent, 2002). The eventual of goal of a insertional mutagenesis screen is to identify the location of the insertions. The genomic junction fragments present as a part of the reads obtained from an insertional mutagenesis screen can be aligned to the genome using BLAT. All alignments with at least a 90 percent match to the genome are

considered. In the event of multiple, the unique best alignment is selected, such that the best alignment is at least five percent better than the second best alignment. IAS uses a dedicated BLAT server for this purpose. Sleeping Beauty screens are no longer limited to mice. Researchers have been using other species like zebrafish, rat and human cell cultures to study cancer using SB screens. In keeping with the demand for multi species functionality, the BLAT server has been loaded with genome databases of human, mouse, rat and zebra fish. At this stage of the analysis we have a list of all the best Sleeping Beauty insertions sites in the host genome.

Annotation

Finally, the aligned sequences are annotated using the UCSC genome annotation databases. Specifically, the refFlat table is used to annotate the integrations with respect to gene, position within the gene, and expected effect given the orientation with respect to the gene. Similar to the BLAT genome databases the annotation databases include refFlat tables for human, mouse, rat and zebrafish and a dedicated server is used to host these databases. Annotations for the genomic fragments from Figure 8 are shown in Figure 9. The annotation file is a tab delimited Excel file containing the listing of all the insertions sites. The first column in the annotation file lists the tumor id followed by the gene name provided the insertion is in a gene. The third column specifies the region of insertion within a gene. The fourth column describes the nature of effect of the insertion. The fifth and the sixth column are the chromosome and the location of the insert on the chromosome in base pairs. The seventh column indicates the number of integrations at this particular position and finally followed by the orientation of the integration in the eighth column. In the annotation files the T() function was used for the gene names. The T() function refers to the text of the value in a field. Some gene names resemble date of the year e.g. Sep1. When excel encounters a gene name like Sep1, it is automatically

converted to 1-Sep as excel assumes it being a date. The T() function leaves the gene name as is in the excel spread sheet to avoid any confusion for the user.

472-4T.parsed		chr7	122388307	6			
472-4T.parsed	Ccr7	3 prime	13.757 kb	chr11	99002634	177	SAME
472-4T.parsed	Bach2	intron 2	not disrupt	CDS chr4	32421757	6	OPPOSITE

Figure 9. The annotations of the genomic junction fragments from Figure 8

Donor chromosomes

The chromosome harboring the original SB cassette is referred to as the donor chromosome. As noted in the Background Chapter, while Sleeping Beauty can transpose to any site (with a TA) in the genome, a substantial proportion of transposition events occur over relatively short distances. This process is termed local hopping. The effect of this process is an abundance of sites on the same chromosome as the donor cassette. These are problematic, as they increase the background number of integrations and will frequently cause multiple CISs and gCISs to be spuriously identified on the donor chromosome. In order to remove the false positives that arise in later analyses (CIS and gCIS) all of the insertions on the donor chromosome are excluded from further analysis. This conservative approach aids in minimizing the false predictions due to local hopping events. Detailed modeling and analysis of local hopping across multiple experiments may eventually allow a more limited set of exclusions on the donor chromosome. The barcode file from Figure 5 indicates that chromosome 4 is the donor chromosome for that particular set of tumors. Therefore, all integrations on chromosome 4 for those tumors are excluded from further analysis.

Clonality

Driver mutations are those mutations that are responsible for tumor initiation and growth. These are expected to be the most prevalently observed integrations within a tumor, as they are clonally selected for during tumor development. The remaining infrequently observed insertions most likely correspond to continued transposition events in the tumor or normal cells that contaminate the tumor samples and were not clonally expanded correspond to passenger mutations. Removing these infrequent insertions will increase the chance of identifying the causal driver mutations (Vrieze et al, In preparation). We have adopted and integrated the technique developed by Vrieze et al (In Preparation) based on the premise that driver mutations will be present across various tumors throughout the animal. They compared the insertion events in thymus and lymph node tumors derived from the same animal. The method defines a metric called the clonality score which is the number of sequences mapped to a particular insertion site from a sample divided by the number of sequences mapped to the insertion site in the same sample with the maximum number of sequences. For a given sample, the integration event with the greatest number of mapped sequences is assigned a clonality score of 1. Vrieze et al (In preparation) observed that integration sites having a clonality score less than 0.1 do not have strong positive selection and therefore defined them as noisy events and eliminated this class of integrations. We have adopted the technique of eliminating the integration events having a clonality score less than 0.1 in the IAS system to eliminate background integration events. Clonality metrics are focused on individual tumors, which make distinguishing passenger mutations from driver mutations a challenge. Such a determination requires an assessment across multiple tumors. The key is that driver mutations, while derived from a diverse population of genes, will be selected for during tumor development. In contrast, passenger mutations are randomly selected in each independent tumor. Thus driver mutations should be observed in

multiple independent tumors. Several methods are discussed that address this important issue.

Common Insertion Sites (CIS)

Common insertion sites (CISs) are defined as regions in which insertions are observed across multiple tumors more often than expected. This is assessed using a Monte Carlo simulation in which the set of integrations, per tumor, are randomly simulated. The set of simulated integrations are restricted to the positions of TA dinucleotides within the reference genome, in keeping with the biology of the SB element. In each iteration, the shortest regions containing integrations (I) from 3, 4, 5, 6 and 7 integrations are identified. These regions are limited to a maximum size of 150 kb, based on transcript length (only 5% of transcripts are longer than 150 kb), to reduce the number of false CISs based upon integrations in disparate, adjacent genes. This set of minimal regions for $I \in \{3, 4, 5, 6, 7\}$ is used to determine the smallest region such that one or fewer CISs would be identified by chance ($E=1$). These definitions are then applied to the experimental data to determine the CISs identified within the experiment. An annotated list of CISs is provided in an Excel-compatible format, including the locus definition, the gene(s) encompassed by the CIS, and the number and identities of tumors in which the CIS was observed.

gene centric Common Insertion Sites (gCIS)

Gene-centric CISs were calculated based upon the number of TA dinucleotides within the transcribed region for each gene in the RefSeq collection (Pruitt, Tatusova, & Maglott, 2006). The gene-associated transcribed region was defined as the union of all RefSeq transcripts including a 10 kbp promoter. A Chi-squared test statistic was calculated based upon the number of TAs within each gene-associated region and the number of tumors with integrations within the gene. This test statistic is used to determine the p-value, with a single degree of freedom. An Excel compatible tab-

delimited file is generated detailing the results. For each RefSeq gene, this file includes the gCIS p-value, number of tumors in which integrations were found, and a list of the tumors in which integrations were observed. Significance was assessed using the Bonferroni method, yielding a threshold of 2.63×10^{-6} to determine which gCISs are significant after correction for multiple hypothesis testing.

In summary, the IAS system takes as input a barcode file containing the necessary parameters and the sequence file itself and returns three files: (i) an annotation file containing the location of all the insertions and their UCSC annotations, (ii) a file containing the data on Common Insertions Sites (CIS), and (iii) a file containing the data on gene centric Common Insertion Sites (gCIS).

IAS Website

To make IAS available to researchers worldwide, it was developed and deployed as a web application to aid in the analysis of insertional mutagenesis experiments. The Drupal content management system was used as the underlying platform upon which the IAS pipeline was deployed as a web application (<http://drupal.org/>). All of the experiment-specific descriptions (metadata) are stored within a MySQL database, with the sequence and barcode files stored within a filesystem hierarchy based upon investigator and experiment name. To enhance the scalability of IAS, the computational analysis is performed on a local compute cluster. The compute cluster is a sixteen node 2GHz AMD Athlon dual processors with 2GB of RAM on each node. All necessary files and commands are transmitted to the compute cluster for execution of the IAS analysis pipeline. Once the analysis is complete the resulting output files are transferred back to the IAS server for access by the investigator. An email is sent to the investigator informing him or her that the analysis is complete.

CHAPTER 5

RESULTS

The IAS website (<http://ias.eng.uiowa.edu/IAS>) provides access to all of the functionality of IAS. This enables SB researchers to rapidly upload and analyze entire experimental datasets. Each researcher's experiments are categorized by name, and are accessible to the researchers individually. The creation of a new project is a straightforward process of uploading the required experimental parameters, and launching the computation. Inputs include: a multi-sequence FASTA file, and a barcode file containing the parameters. The barcode file shown in Figure 5 provides the per-tumor information required to identify the integration junction sites. For each tumor, this information includes the associated barcode, cloning orientation (IRR or IRL), expected flanking sequences and donor chromosome are specified. Template barcode files are available to ensure proper exchange of information.

The screenshot shows the IAS login page. At the top, there is a yellow header bar with the text "Integration Analysis System" and a "Contact" link. Below the header, the page is divided into a grey sidebar on the left and a white main content area. The sidebar contains the "User login" section, which includes a "Username: *" field with the text "arnold", a "Password: *" field with masked characters, a "Log in" button, and two radio button options: "Create new account" and "Request new password". The main content area displays "Welcome to IAS" and a subtitle: "A Bioinformatics system for insertional mutagenesis analysis of Sleeping Beauty models of cancer".

Figure 10. IAS login page

The users are first required to request a login and the administrator approves the registration. The users can then login to create an experiment as shown in Figure 10. Every dataset that needs to be analyzed is considered an experiment and the users are required to give an experiment name and specify the location of the barcode file and the sequence file to be uploaded on the “Add Experiment” page as shown in Figure 11. The users are also required to specify the host organism in which the SB screen was performed.

The screenshot shows the 'Create Experiment' page in the Integration Analysis System. The page has a yellow header with the University of Iowa logo and navigation links: 'Add Experiment', 'Contact', 'My Integrations', and 'Log out'. A left sidebar shows the user 'tomic' with options for 'My account' and 'Log out'. The main content area is titled 'Create Experiment' and includes a 'Title' input field, a 'Species' dropdown menu (with options Human, Mouse, Rat), and two file upload sections: 'Barcodes' and 'Sequences'. Each upload section has a 'Browse...' button, an 'Upload' button, and a 'Maximum Filesize: 1000 MB' limit. A note states: 'The barcodes file should be a tab delimited description of the barcodes.' Below the upload sections is a text field for 'Location of the 454 sequence run file.' At the bottom are 'Save' and 'Preview' buttons.

Figure 11. IAS page where the title of the experiment, the host organism are specified and the barcode file and the sequence file are uploaded to the IAS server.

IAS supports the analysis of SB experiments in mouse, human, rat and zebra fish. Pressing the Save button on the “Create Experiment” page initiates the analysis. Because insertional mutagenesis experiments involve large datasets, the complete analysis requires from a few minutes to several hours depending on the size of the dataset. The users can choose to leave the browser open or quit. Regardless the analysis will continue to run. Once complete the users will be notified by email of its completion and the user

can view the results on the “My Integrations” page on the website as shown in the Figure 12. The My Integrations page lists all the experiments of a particular user along with the Inputs Barcodes file, Sequence file and the results of the analysis being the Annotation file, CIS and gCIS files. The webpage also has a delete link to delete a particular experiment. Finally the users can exit IAS by logging out of the website.

As shown in Figure 3, sequences are first classified into tumor of origin based upon the oligo-nucleotide barcode incorporated within the sequences. Non-genomic flanking sequences are then removed. These include the inverted repeat from the SB element at the 5' end and any adaptor sequence found at the 3' end of the read. The remaining sequence now represents the genomic sequence immediately adjacent to the SB integration, including the TA site. This sequence is then mapped to the reference genome assembly. The set of integrations for each tumor are then annotated to include any gene in which it integrated, and the expected effect of the integration on the gene given the relative orientation of the gene and SB element. The annotation file also includes the number of integrations observed at a given position. This information is used to identify Commonly Integrated Sites (CISs) and gene-centric Commonly Integrated Sites (gCISs).

Resulting output files of an analysis by IAS

The outputs of the IAS analysis are several files, all available from the web-site. These files include the annotation for every integration, as well as descriptions on the common integrations sites and gene-centric common integration sites. The files are provided in a tab-delimited, Excel-compatible format to maximize their utility to the users of IAS.

The screenshot shows the 'My Integrations' page on the IAS website. The page has a yellow header with the University of Iowa logo and navigation links. The main content area contains a table with the following data:

Title	Barcodes	Sequences	Inserts	CIS	CIG	Delete link
Human_IRR_V3	IRRHaCatBarcodes_0.txt	2.TCA_454Reads.fna_0.txt	Annotation_0.xls	CIS_0.txt	CIG_0.txt	delete
Human_IRL_V3	IRLHaCatBarcodes_0.txt	1.TCA_454Reads.fna_0.txt	Annotation_0.xls	CIS_0.txt	CIG_0.txt	delete
Human_IRR_v2	IRRHaCatBarcodes_0.txt	2.TCA_454Reads.fna_0.txt	Annotation_0.xls	CIS_0.txt	CIG_0.txt	delete
Human_IRL_v2	IRLHaCatBarcodes_0.txt	1.TCA_454Reads.fna_0.txt	Annotation_0.xls	CIS_0.txt	CIG_0.txt	delete
Human_IRL	IRLHaCatBarcodes_0.txt	1.TCA_454Reads.fna_0.txt	Annotation_0.xls	CIS_0.txt	CIG_0.txt	delete
devel_test20	barcodes_0.txt	1.TCA_454Reads_0.fna	Annotation_0.xls	CIS_0.txt	CIG_0.txt	delete
devel_test19	barcodes_0.txt	1.TCA_454Reads_0.fna	Annotation_0.xls	CIS_0.txt	CIG_0.txt	delete
devel_test5	barcodes_0.txt	1.TCA_454Reads_0.fna	Annotation_0.xls	CIS_0.txt	CIG_0.txt	delete
kis2	barcodes_0.txt	1.TCA_454Reads.fna_0.txt	Annotation_0.xls	CIS_0.txt	CIG_0.txt	delete
kis1	barcodes_0.txt	1.TCA_454Reads.fna_0.txt	Annotation_0.xls	CIS_0.txt	CIG_0.txt	delete

At the bottom of the table, there is a pagination control showing '1 2 3 4 5 6 7 8 9 ... next > last >'.

Figure 12. Screen shot of the listing of all the input and results on the My Integrations page on the IAS website

Annotation file

The annotation file is a tab delimited, Excel-compatible file containing the listing of all insertions sites. The first column in the annotation file lists the tumor id followed by the gene name if the insertion is in a gene. The third column specifies the region of insertion within a gene. The fourth column describes the nature of effect of the insertion. The fifth and the sixth column are the chromosome and the location of the insert on the chromosome in base pairs. The seventh column indicates the number of integrations at this particular position and finally followed by the orientation of the integration in the eighth column. In the annotation files the T() function was used for the gene names. The T() function refers to the text of the value in a field. Some gene names resemble date of the year e.g. Sep1. When Excel encounters a gene name like Sep1, it is automatically converted to 1-Sep as Excel assumes it being a date. The T() function leaves the gene name as is in the Excel spread sheet to avoid any confusion for the user.

Common Insertion Sites (CIS) file

Every entry in the CIS file starts with the CIS definition, which the chromosome number and the beginning and the end of CIS on the chromosome followed by the number of independent insertions, genes in the neighborhood of the CIS and finally the tumors with insertions in this neighborhood.

gene-centric Common Insertion Sites (gCIS) file

The gCIS file includes the listing of all the genes in the genome with the P-values indicating the significance of the number of tumors with insertions in that gene plus a 10000bp promoter and the listing of the tumors. Just like the annotation file and the CIS file the gCISs are also presented as a tab delimited excel spreadsheet. Since the gCISs are gene centric the first column in the gCIS file is a gene name followed by the Chi-Squared value Degrees of Freedom in the second column. The third and the fourth columns in the gCIS file are the q-value and p-value. The fifth, sixth and the seventh columns are number of tumors with insertion in this gene, number of integrations per tumor and the tumor ID's respectively.

Support for analyzing SB experiments from multiple species

IAS includes analysis for multiple species like mouse, human, rat and zebrafish using SB system for insertional Mutagenesis.

Experimental results

The IAS system has been used in the analysis of multiple experiments ranging from lymphoma, and colorectal cancer to medulloblastoma. The following is a summary of the IAS analysis from those experiments. Table 1 summarizes each experiment analyzed using IAS. It lists the tumor type, number of sequences and tumors analyzed, and the CISs and gCISs identified.

Experiments	Sequences	Tumors	CIS	gCIS
Medulloblastoma	635015*	125	219	191
Metastatic Tumor	635015*	170	197	159
Colorectal	196619	135	84	324
Lymphoma	625286	161	71	221
Total	1456920	591		

*The Medulloblastomas and the Metastatic tumors are paired

Table 1. Summary of experiments analyzed using IAS

We have analyzed a total of approximately 591 tumors from three different types of experiments involving approximately 1.4 million sequences.

Detailed analysis of the lymphoma dataset

Sequence data from three models of thymic lymphomas in mice from Vrieze et al (In preparation) has been analyzed by the IAS system. The goal of this project was to identify distinct genetic signatures of various cells of origin for T-cell lymphomas. The T-cells have their origin in hematopoietic stem cells in the bone marrow. These T-cells reside in the thymus and by subsequent cell divisions become immature thymocytes with no expression of either CD4 or CD8 antigen. These thymocytes in the later stages of development become mature by the expression of CD4 and CD8. The SB system in each of these models is engineered to be triggered in specific cells during these various stages

	Vav	Lck	CD4
Number of Tumors	36	28	48
Sequences Mapped	56,926	56,926	105,366
Unique Integration sites	837	922	1830
Sites observed in 2+ tumors	8	2	6
Sites Observed in 3+ tumors	4	0	2
Number of CISs	17	19	35
Number of gCISs	28	52	141

Table 2. The summary of results from the analysis of Vav, Lck and CD4 models of lymphoma at different stages of the analysis

in differentiation of the T-cell. In the Vav model, transposase is expressed using a promoter specific to hematopoietic stem cells. Similarly, in the Lck model SB transposase is expressed in thymocytes lacking the CD4/CD8 antigen. Finally, the CD4 model of lymphoma uses a promoter, which expresses SB transposase in late stage CD4/CD8 double positive thymocytes (Vrieze et al. In preparation). The identification of the underlying genetic signature of the cell of origin is important to distinguish the normal cells from the malignant ones. This experiment is an attempt to identify the genetic events in cell of origin by using SB mediated insertional mutagenesis activated at different stages of the development and differentiation of the T-cells that eventually become cancerous. Identifying the genetic events and the stage of cancer initiation is necessary for effective drugs and therapy.

The dataset involved a total of 112 tumors. The complete description of the dataset and its analysis is shown in Table 2. In summary, there were 36 tumors from the Vav model, 28 tumors from the Lck model, and 48 tumors from the CD4 model. IAS successfully mapped a total of 56,926 reads from the Vav model, 56,926 reads from the

Lck and 105366 reads from the CD4 model to the mouse genome corresponding to 837, 922 and 1830 independent integrations sites. These independent integrations from the annotation files of each of the Vav, Lck and CD4 models are used to calculate the CIS and gCIS for each of the models. The IAS system Identified 17, 19 and 35 CIS for Vav, Lck and CD4 tumors respectively. The listing of the CISs for Vav, Lck and CD4 tumors is listed in Tables 4, 5, 6 of APPENDIX A. Table 2 also gives the number of integrations sites observed in at least 2 and 3 tumors.

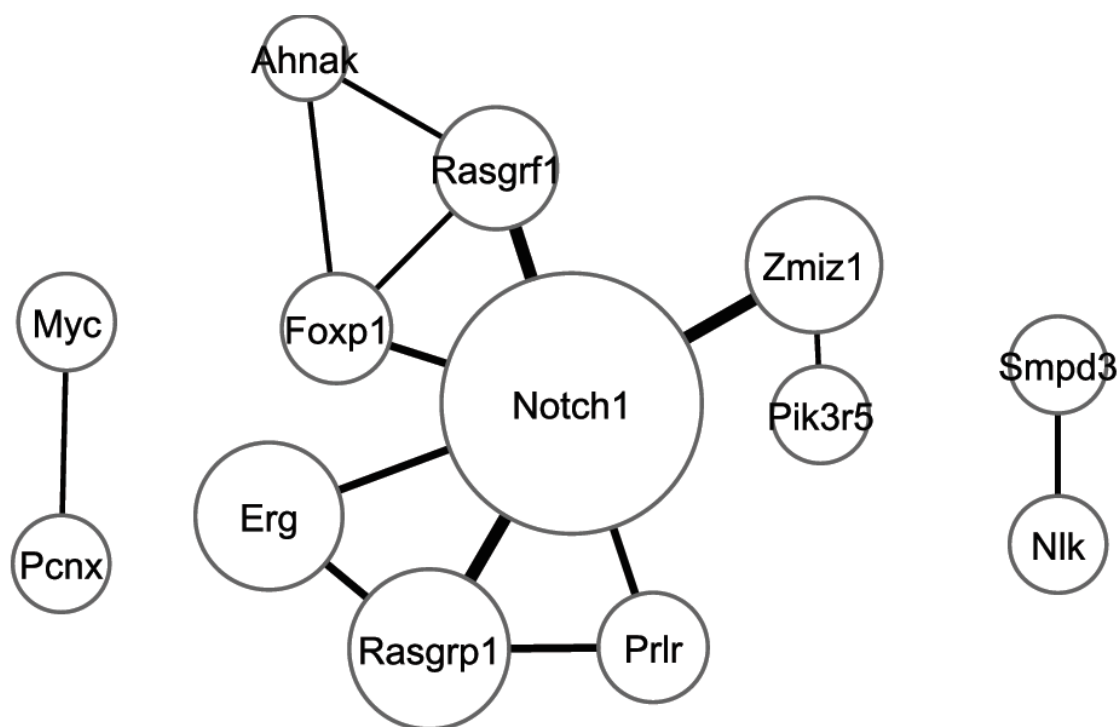


Figure 13. Pathway observed in Vav model of Lymphomas in mice

The set of gCISs for each of the lymphoma models was analyzed, as described in the Methods. Overall, 31, 54 and 142 gCISs were identified from the Vav, Lck and CD4 tumor models, respectively. The significance of this analysis was adjusted for multiple hypothesis testing using a Bonferroni correction. The top twenty gCISs ranked based on

the unadjusted p-value from the χ -square test for the SB mediated lymphoma models of Vav, Lck and CD4 are listed in Tables 7, 8, 9 of APPENDIX A. Several analyses were performed on the sets of identified CISs and gCISs to assess their relevance and correlate them with the biology of lymphoma. The first analysis was a comparison between the CISs and gCISs to databases of known cancer genes. This analysis identified a significant overlap. Vrieze et al, (In Preparation) performed a genome wide analysis of Human T-ALL samples in identifying 31 copy-number abnormalities (CNAs) of which 10 were amplification events spanning 4850 genes and 21 deletion events affecting 513 genes. Mouse orthologs for the genes within the CNAs were identified and were compared against the set of genes within the CISs and gCISs from the three models. Vrieze et al (In Preparation) observed a statistically significant overlap between the two. Thus indicating that SB mediated screens in mice can be a potential system to simulate and understand human cancer.

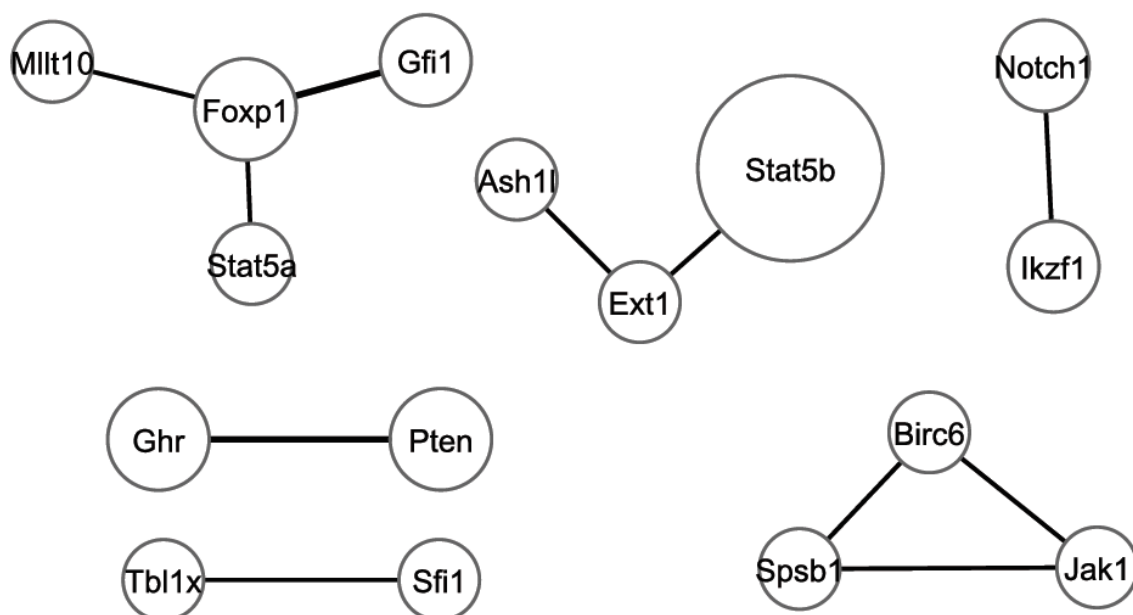


Figure 14. Pathway observed in Lck model of Lymphomas in mice

As described in the Background chapter of this thesis, cancer is caused by mutations in multiple genes in critically important pathways. Cooperatively, these genes are responsible for tumor initiation and progression. These genes are hereafter referred to as cooperating genes. So an effort was made identify these cooperating genes. A Fisher's exact test was performed on the CIS/gCISs pairs from each of the three models (Vav, Lck and CD4) of SB to identify possible cooperating pair of genes. The results of the Fisher's exact test for the Vav, Lck and CD4 tumors are furnished in Tables 10, 11, and 12 respectively in APPENDIX A. There are 3, 8 and 4 gene pairs that show significant interaction from Vav, Lck and CD4 models respectively. The relatively low numbers of identified cooperating gene pairs can be attributed to a limited number of tumors for each model. An effort was made to identify cooperating gene networks beyond gene pairs. A software application called Cytoscape (Shannon et al., 2003) was used to study cooperating genes in the three lymphoma models. The gene networks for each of the models are shown in Figures 13, 14, 15. In each of these figures, each node represents a gene, a node's diameter is proportional to the number of tumors in which the gene had observed integrations, and edge thickness is proportional to number of tumors that have an insertion in both genes connected by the edge. It evident from Figures 13,14,15 that the mutation profiles are different for the three different models of Vav, Lck and CD4, suggesting the cell of origin is an important factor in the genetic selection of tumors (Vrieze et al, In Preparation). The mutation patterns of CD4 and Vav models differ the most. *Notch1*, *Ikzf1*, *Foxp1*, *Erg* and *Rasgrf1* harbor insertions in Vav model but are absent in the CD4 model, Whereas *Whsc1*, *Jak1* and *Gfi1* harbored mutations in the CD4 model (Vrieze et al, In Preparation). Specifically, the gene-interaction network from the Vav-derived tumors in Figure 13 exhibits the least complexity and the most robust roles for specific genes. Clearly, given the size of the node representing *Notch1*, integrations therein are observed more frequently than any other gene in the Vav model. Many of the other most frequently integrated genes are found in combination with *Notch1* (*Rasgrf1*,

Rasgrp1, *Zmiz1*, *Pik3r5*). These genes possibly cooperate with Notch1 to develop Lymphomas triggered by *Notch1*. Recent studies have shown that the *Notch* and *Ras* (*Rasgrp1* and *Rasgrf1*) pathways cooperate to induce T-cell Lymphomas in mice (Vrieze et al, In Preparation). This set of genes is a minor constituent within the gene-interaction network for Lck, shown in Figure 14. In this network, the number of significant genes is approximately equal, however there is no evidence of a “hub” node such as Notch1 in the Vav-derived network. Although Notch1 is present in the Lck-derived network, it is relegated to a significantly smaller role.

Finally, the CD4-derived network is substantially larger than the Vav- and Lck-derived networks. Similar to the Vav network, it appears to have several “hub” nodes – *Myc*, *Gfi1*, *Whsc1*, *Akt2*. However, many of the hub-interacting genes appear to interact with a single hub. These different hubs possibly indicate different mutation profiles in the CD4 model. Tumors in the Vav model initiated in the Hematopoietic stem cell are less complex than their more differentiated counterparts in the CD4 model. The tumors in Vav appear to primarily driven by *Notch1* where are the tumors in CD4 model are increasingly heterogeneous (Vrieze et al, In Preparation).

Colorectal cancers

The previous analysis demonstrated the application of IAS in analyzing SB mediated models of Lymphomas in mice. The goal of this analysis is to compare our CIS method with the one from Starr et al (Starr et al., 2009). This experiment utilized SB induced insertional mutagenesis in mice to identify genes involved in colorectal cancers. In all, Starr et al. sequenced 135 tumors, identifying 77 CISs involved in colorectal cancer. There are 106 genes total within these 77 CISs identified by Starr et al. In contrast, IAS identified 84 CISs having 116 genes within these CISs listed in Table.13. and 324 gCISs shown in Table 14 of APPENDIX A. There are 74 genes in common

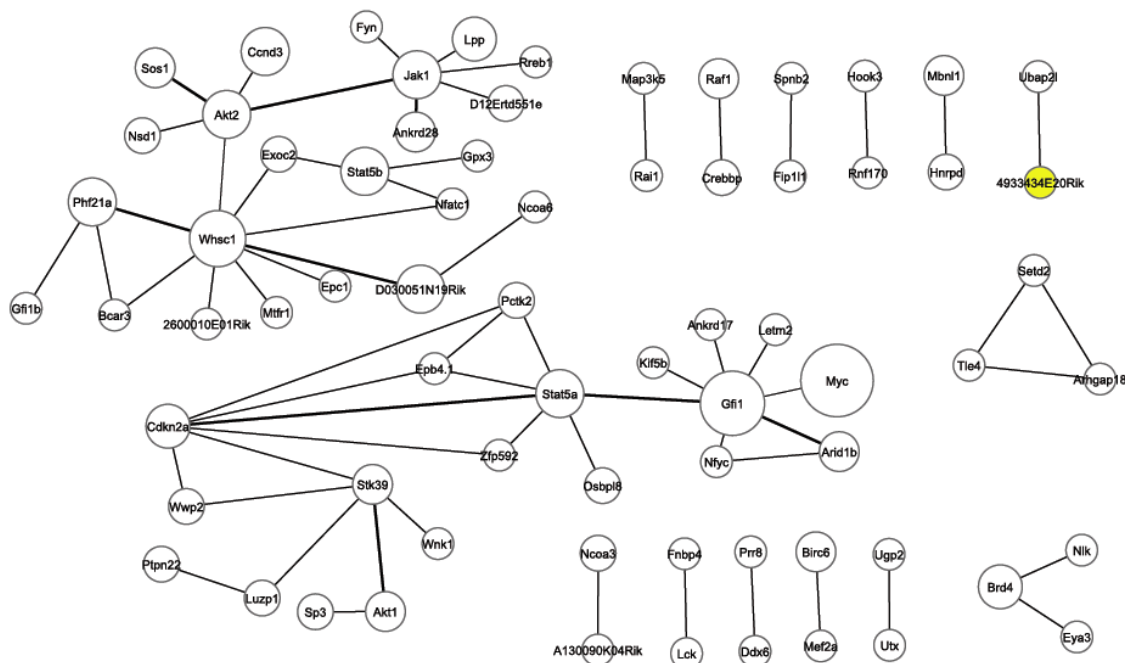


Figure 15. Pathway observed in CD4 model of Lymphomas in mice

between the lists of genes within the CISs Identified by our method and Starr et al. From Figure 16, overall there is an overlap of 54 genes between the CISs, gCISs of our method and CISs method by Starr et al.

Medulloblastomas and associated metastatic spine tumors

A set of 125 medulloblastoma tumors along with 170 of their metastatic spine tumors, comprising a total of approximately 600,000 have been analyzed using IAS. IAS identified 219 CIS and 191 gCIS for the medulloblastoma and 197 and 159 for their associated metastatic tumors. An analysis to identify cooperating gene pairs using fishers exact test was also performed.

Various other analyses were also performed using IAS involving SB mutagenesis human cell lines, zebra fish and rat.

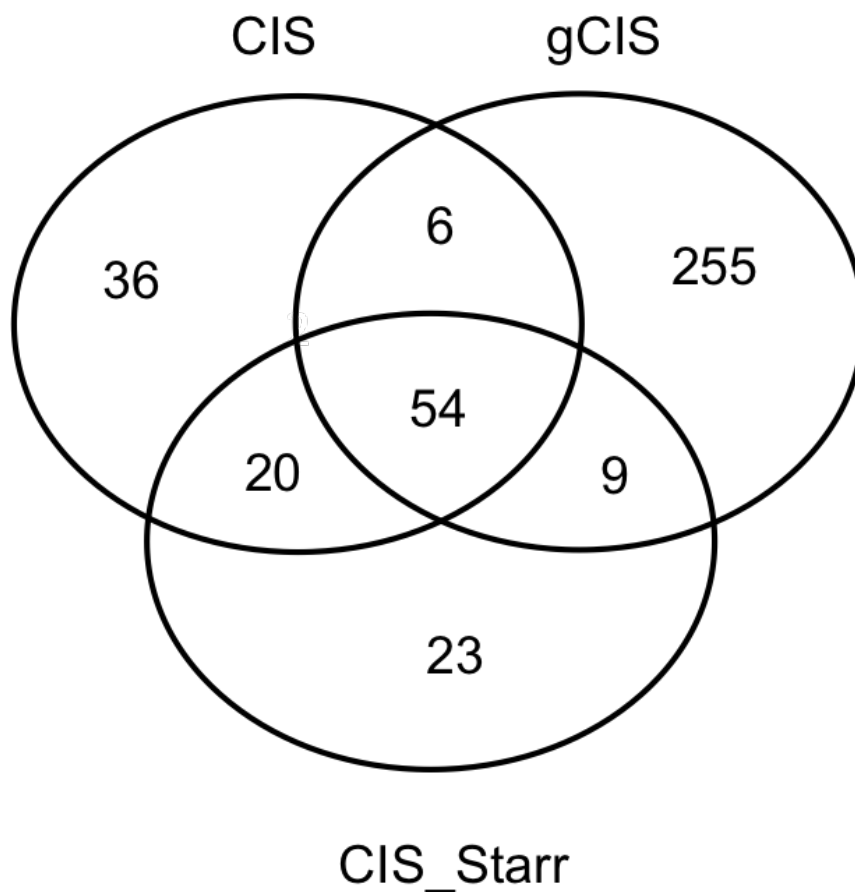


Figure 16. The extent of overlap between CIS, gCIS identified by IAS and CIS identified by method specified in Starr et al.

Skin and Liver tumors

An experiment to test the efficacy of Sleeping Beauty transposon system in mice to induce Skin and Liver tumors was conducted. The SB system was successful in generating HCC and SCC tumors in mice. The sequences resulting from 12 liver tumors and 18 skin tumors were analyzed. The sequences resulting from 12 liver and 18 skin tumors were mapped to 1821 and 3129 unique integration sites. Further analysis of the 1821 integration sites from liver tumors resulted in 5 CIS and 13 gCIS listed in Tables

15 & 16 of APPENDIX A. Similarly the analysis of 3129 integration sites from skin tumors resulted in 5 CIS and 3 gCIS listed in Tables 17 and 18 of APPENDIX A.

CHAPTER 6

DISCUSSION

Some issues, concerns encountered during the design and implementation of IAS along with possible enhancements are detailed in this section. This section addresses the pros and cons of barcode design with respect to the experiment at hand and the sequencing platform. An evaluation of the software packages for removal of flanking sequences is also presented. The effect on IAS from changing genomic builds and annotation is discussed. A comparison of IAS's CIS method is compared with other existing CIS algorithms. Finally the effect of existing and future sequencing technologies vis-à-vis the design of IAS has been detailed in this section.

Barcode design

The barcode design strategy utilizes oligonucleotide barcodes to uniquely identify each tumor from within a heterogeneous mixture of sequences. This allows large-scale pooling of tumors within a single high-throughput sequencing experiment. Such pooling enables efficient utilization of the underlying sequencing platform. The barcodes themselves may be re-used across experiments, such that each barcode uniquely identifies a single tumor in any single experiment. Although many of the next-generation sequencing platforms incorporate the ability to pool samples, their ability is typically limited to a modest number and have not been rigorously designed to exhibit robust barcode identification in the presence of sequencing errors. In contrast, the current set of barcodes utilized in our experiments contains 288 barcodes. This set of barcodes was designed using UITagCreator (Gavin et al., 2002) such that all barcodes are at least edit distance 3 and Hamming distance 5 apart. This allows the detection and correction of a single indel or up to two substitution errors within the barcode. Because different sequencing platforms have different error models, it may be beneficial to develop

barcode sets specific to each platform. For example, the likelihood of an insertion or deletion on the 454 model is high in comparison to the Illumina and Solid platforms, particularly when runs of the same nucleotide is present. Therefore, a 454-specific design criteria might incorporate the requirement that mononucleotide runs are limited to two (or even one) nucleotides.

The barcodes currently utilized are ten nucleotides long. Multiple experiment parameters affect the optimal barcode length. Longer barcodes can allow larger numbers of samples to be simultaneously pooled. Similarly, increasing the length of barcodes may also enable more robust error correction properties. The downside of increasing barcode length is two-fold: (i) decreasing sequence length after removal of the barcode sequence, and (ii) an increase in the cost of the primers needed to create the library. The primer cost difference is minimal, however the number of net (i.e., mappable) nucleotides per sequence can be an issue when utilizing short-read platforms such as the Illumina and SOLiD™ platforms.

Removing the flanking sequences of the genomic junction fragment

A variety of alternatives were carefully considered before `cross_match` was selected as the program of choice to remove the flanking sequences of the genomic junction fragment. The previous version of IAS used BLAST (Kent, 2002) as a means to remove the flanking sequences. Using BLAST to remove flanking sequence required aligning the reads against the database of the flanking sequences and subsequently parsing the results. This process involved dealing with a large number files as the sequence file was split into individual FASTA files, each containing a single sequence. Each of these files was aligned to the possible flanking sequences and based on

the match they were removed from the original sequence. This approach was not particularly feasible with next-generation sequencing technologies as they generate numbers of reads in the order of hundreds of thousands to millions.

An alternative option was `vectorstrip`, another popular program for removing vector sequences surrounding sequence of interest. It is a part of the EMBOSS suite of software (Rice, Longden, & Bleasby, 2000). Given a list of input sequences and list of vector sequences `vectorstrip` searches the input sequences for contaminating vector sequences and removes them. The flanking sequences of the genomic junction fragments resulting from SB screens are analogous to the vector sequences intended for removal using `vectorstrip`. Initially `vectorstrip` was seriously considered to be used to remove the genomic junction flanks but was later dropped. While `vectorstrip` efficiently removes the flanking sequences, even in the presence of substitution errors, it fails completely in the face of insertion and deletion errors. This resulted in discarding some genuine genomic fragments in the presence of single insertion or deletion errors.

`cross_match` was considered the ultimate fit for the task as it takes care of both the nucleotide mismatches as well as insertions and deletions caused due to errors in sequencing. In addition, newer versions of `cross_match` have been updated to accommodate the millions of reads resulting from next-generation sequencing platforms.

Local hopping

IAS requires that users specify the donor chromosome as a parameter in the barcode file and removes all the integration events on the donor chromosome from the annotation file when identifying CISs and gCISs. Since there are no established techniques to estimate the extent of local hopping in SB mediated mutagenesis, we rely on removing all integration events on the donor chromosome even though it is extremely conservative.

While this is extremely conservative, it ensures that no inappropriate CISs or gCISs are identified. To compensate for the lack of an entire chromosome, experiments typically use organisms (mice) derived from one of two donor chromosomes. Thus, the power to detect events on the donor chromosomes is reduced, but not entirely absent.

Standard annotations

IAS addresses two of the most common challenges in genomic science. The need to accurately, rapidly and consistently annotate the resulting data, and the need to migrate such results from one genome build to another. Providing the resulting annotation in a standardized format, regardless of genome build or annotation source, is absolutely required to utilize the data in further analyses (e.g. determining CISs and gCISs). Similarly, providing annotations based upon consistent and up-to-date genome builds is a recurring challenge in many experiments, in which the underlying reference sequence and therefore it's associated annotation (e.g. genes) change from build to build over the course of years. Because of this issue, data sets predicated upon position data are not reliable for inter-build comparison. Even gene-based datasets may not provide an accurate basis for comparison, due to the fluid definitions of the reference genome and of the transcripts themselves.

As increasing amounts of data are made available, the reference genome and reference transcriptome improve. This is a good thing. But the dynamic nature of these references makes comparisons between different experiments challenging. It is critical that all analyses within a given analysis must be analyzed relative to the same annotation set (set of genes and the reference sequence).

Comparison of CIS identification strategies

Several groups have developed methods for identifying CISs (De Ridder, Uren, Kool, Reinders, & Wessels, 2006). These vary depending upon the assumed distribution to be sampled, the underlying statistical method (or lack thereof).

The CIS method requires integrations from a minimum of three tumors. This requirement safeguards from a potentially large number of false CISs due to a low level of inter-sample contamination. We have noted that a significant preponderance of CISs derived from two tumors derive from integrations at the exact same position, but with radically altered prevalence between the tumors.

This datum raises the concept that not all integrations sites should be considered equally. In fact, given a reasonable sequencing depth (say several hundred sequences per tumor), integrations that are observed a single time are virtually guaranteed to be present in only a small percentage of tumor cells. Such integrations are thus unlikely to represent initiating or progression events (i.e. are not clonally expanded). Statistical methods are needed to robustly categorize integrations as clonal or non-clonal. Such methods would allow the incorporation of CISs supported by two tumors, increasing the genetic complexity supported by such methods.

General utility

While the IAS system has been motivated primarily by the need to analyze Sleeping Beauty experiments, it is capable of analyzing data many other experiment types. Specifically, the computational pipeline within IAS can be used to map and annotate any sequences that are tagged and flanked by known sequence on both ends. These include PCR generated products, or sequences isolated from a variety of other molecular protocols. The only limitations are those imposed by the alignment algorithm and the length of genomic sequence available. These factors are primarily an issue when the genomic sequence (after removing the flanking sequence) is short. Unsurprisingly,

shorter sequences are less likely to have unique best alignments to the genome. In addition, BLAT is designed to identify sequences with 95% similarity or more with the length of the sequences being at 40 base pairs.

Thus IAS may be used to map sequences from other transposon and vector-based integration systems. Of note, however, the CIS and gCIS methods would produce inaccurate results, as the TA-integration assumption would not be valid for those systems. IAS could also be used to perform a preliminary analysis of mRNA-based sequencing (i.e. ESTs) to perform preliminary expression level and gene classification. Such results would require additional processing of the annotation file to identify transcript structures.

Beyond 2nd generations sequencing technologies

Technology	Roche 454	Illumina Solexa	ABI Solid	Capillary
Run Cost	\$10,000	\$4,000	\$8,000	\$144
Read Length	300-400	75-100	50	400-800
Number of Sequences	400,000	40,000,000	80,000,000	96

Table 3. Comparison of different sequencing platforms based on their read length the number of sequences they generate and the run costs

Availability of third generation sequencing technology will further benefit Sleeping Beauty research, but carries with it additional challenges. The challenges associated with these platforms relate to sequence length and the number of sequences available from a given experiment.

As shown in Table 3 the currently available “short-read” sequencing platforms such as the Genome Analyzer Iix (Illumina) and SOLID (ABI) both are capable of generating extremely large numbers of sequences. Experiments utilizing these platforms can result in hundreds of millions of sequence reads of 50-100 nt in length as show in the Table 3.

Sequencing technologies are evolving at a rapid rate. The initial implementation of IAS was developed for capillary-based sequencing experiments involving hundreds of sequences, and has been extended to accommodate analysis of next-generation sequencing (e.g., the Roche/454 FLX) technologies resulting in hundreds of thousands of reads. Most recently investigators have begun using the Illumina platform, generating tens of millions of reads for each experiment. Efficiently mapping such reads requires a different strategy. Although BLAT suffices for experiments with millions of sequences, it becomes a bottleneck when analyzing orders of magnitude greater number of reads. Given a nominal throughput of 1M mapped reads for two hours for BLAT, the expected time to map 1 billion reads is 2000 hours. For this reason such experiments require next-generation sequence alignment software. Many programs exist for these purposes, including Bowtie (Langmead, Trapnell, Pop, & Salzberg, 2009), Maq (H. Li, Ruan, & Durbin, 2008) and Mosaik (Hillier et al., 2008).

The other challenge with migrating to these next-generation sequencing platforms is the limitation imposed by the read-length. Between the oligonucleotide barcode used to identify the tumor, and the partial sequence of the inverted repeat necessary for molecular isolation of the genomic junction fragments, at least 30 nucleotides of any sequence does not represent the desired sequence. After these pieces have been removed the remaining sequence may be too short to unequivocally/uniquely map to the genome. This is

particularly true, as the error rate typically increases as the read length increases. In fact, this particular experimental reality effectively excludes the current generation of ABI SOLiD sequences for SB experiments. With a current limit of 50 nt, the resulting 20 nt fragments (maximum) are far too short to yield unambiguous mapping locations for the majority of integration sites.

These technologies will allow unprecedented sequencing depth of SB induced tumors. This is important, as the population of integrations within a tumor are not all clonal. In fact, given the heterogeneous mix of cells within a tumor, it is often challenging to determine whether a given integration site is biologically relevant to the development of the tumor (i.e., clonally expanded within the tumor) or merely a random event in a small population of cells.

Improved determination of clonality is expected to allow insight into the processes underlying tumor development. For example, genes that fall into the sub-clonal category may be those that aid in tumor growth but are not required for tumor initiation. The number of tumors to be sequenced may also be increased, as the sequencing depth will no longer be limiting with these newer platforms. This increase in number of tumors and sequences will help in inferring the complex genetics underlying tumor formation, development and metastasis. While a dozen (11-17) genes must be mutated, they are derived from an estimated population of dozens to hundreds of genes (71 colorectal; 122 breast; Wood et al. 2007). Not all combinations of mutations will be sufficient to cause tumors, but the investigation of the complex genetics is likely to require several dozen, if not hundreds, of independent tumors.

Given sufficient depth of sequencing, future experiments should be able to predict the order in which mutations have occurred. More recent mutations will be present in a

sub-population of the tumor and thus should be observed less prevalently than initiating or driving mutations.

CHAPTER 7

FUTURE WORK

Future work on IAS will focus on making the system more accessible and useful to investigators. Included in this effort is improved reporting of QC metrics for each step of the analytic pipeline (e.g. number of sequences per tumor, number of sequences per tumor that align to the genome). This data will be presented for entire experiments and for individual tumors. Such metrics enable investigators to evaluate the preparation of specific tumors, or with their overall protocol.

Although the majority of Sleeping Beauty research to date has utilized the laboratory mouse, nothing prohibits utilizing this system to study cancer in other organisms. The only requirements are a donor site with a cassette of SB elements and a SB transposase under the transcriptional control of a functional promoter. To date, the SB system has been utilized in mouse, rat (Lu et al., 2007) and zebrafish (Davidson et al., 2003), and is likely to be utilized in other organisms – including human tissue cultures. IAS has been extended to include the analysis of insertional mutagenesis experiments using the SB system in mouse, rat, zebra fish and human tissue cultures. Extending IAS to allow analysis versus multiple organisms is virtually identical to supporting multiple reference genomes within a single organism. This capacity will allow comparison to previously reported results that may be difficult, or even impossible to replicate/validate among different reference genomes.

SB elements transpose both globally (i.e., between chromosomes) and locally. The prevalence of local re-integration (local hopping) makes identification of CISs and gCISs near the SB cassette challenging. The current implementation of IAS addresses this challenge by excluding the entire donor chromosome from further analysis (for each tumor). While effective, this method is overly conservative. Another piece of future work is to develop a strategy based upon the known properties of SB transposons –

specifically, their propensity for “local hopping”. One strategy to account for an observed bias of integrations near the donor cassette is to empirically determine the overabundance of integrations. With such a strategy, the significance of integration clusters (CISs or gCISs) are determined based upon deviation from the expected distribution away from the site of the SB cassette.

A value-added annotation that will be incorporated into IAS is the prediction of gene effect – is the gene likely to be an oncogene or a tumor suppressor? Previous results have shown that SB integrates throughout tumor suppressor genes in both orientations. In contrast, the pattern of SB integration within oncogenes is often restricted to a limited number of sites/regions within the transcript all with the same orientation. In this way, the exogenous promoter within the SB element can drive expression of the gene (or a fragment thereof).

The main concentration of IAS has been to identify genes involved in cancer. New research points to the involvement of ncRNA as well. Some micro RNA have been associated with various types of cancer (Meltzer, 2005). A cluster of mir-17-92 micro RNA have been observed to be substantially amplified in B-cell lymphomas when compared to normal cells (He et al., 2005). To realize the full potential of SB mediated insertional mutagenesis there is a need to look beyond protein-coding genes and their promoters.

Although Sleeping Beauty overcomes various limitations of viral-mediated insertional mutagenesis it has its share of limitations. The most significant of which is local hopping - the tendency of transposons to re-integrate in the proximity of the donor site. This phenomenon can result in false CISs on the donor chromosome. To alleviate such local-hopping-derived false CISs, IAS removes all the integrations from the donor chromosome when analyzing integrations for CISs and gCISs. Removing the entire donor chromosome in identifying CISs and gCISs may be extremely conservative. As more and

more researchers look toward SB for their insertional mutagenesis there is a necessity to develop method to estimate the effect of local hopping and include it into the IAS system.

Future extensions to IAS should include the ability for the user of IAS to be able to access data across experiments. The annotation file currently is stored on IAS server in a tab delimited text format. A database has to optimally designed to hold all the annotation data on IAS and give the user of IAS the ability to query across their experiments on the basis of gene, locus, experiment or position etc. This will give the user an opportunity to take a holistic approach across experiments in understanding cancer. This type of meta-analysis can lead to identification of significant cancer gene networks and mutation profiles of the particular tumor under study.

With the advent of new genome sequence technologies and the staggering amounts of data they generate there is a need to look beyond identifying CIS/gCISs and more towards genetic networks. The systems approach as in Vrieze et al. 2010 (In Preparation) elucidate the distinct genetic signatures of the tumors based on the cell of origin, thus facilitating an appropriate therapy, drugs or a combination of both in future. Although there is significant work before we can actually customize drugs and therapy based on the cell of origin or genetic makeup of the individual, careful design of experiments and databases now can facilitate such a possibility in the future. The identification and graphical representation of the genetic networks based on SB data should be made a part of the analysis pipeline.

As mention in the earlier chapters of this thesis cancer is caused by an initiating mutation followed by clonal expansion and one of those cells acquiring another mutation and so on. Understanding the order of these mutations is important to understand the cause, progression and possible cure for cancer. Vrieze et al. 2010 (In Preparation) is a right step in that direction and answers a tiny part of the question, more needs to done in terms careful design of the experiments by experiments biologists and computational techniques by computational biologists.

Sleeping Beauty mediated mutagenesis can both drive the expression of genes as well as truncate the transcript based on its location vis-à-vis the gene. IAS needs to incorporate this particular piece of information for every insertion in the annotation files based on the location and orientation of SB integration.

In summary, Sleeping Beauty mediated mutagenesis is a very potent tool in the realm of insertional mutagenesis. SB screens coupled with next-gen sequencing technologies provide a unique opportunity for researchers to better understand cancer initiation, progression and metastasis. IAS provides the necessary analysis for experimental biologists to analyze the data from their SB screens and more and more analysis are yet to be included into IAS. IAS caters and continues to cater to the analytical needs of the scientific SB community and aid them in understanding cancer.

APPENDIX

Table A1. Common Insertion Sites (CIS) resulting from the Vav model of Lymphoma in mice.

Locus	Gene
chr15:61815526-61816594	
chr7:28389685-28390957	Akt2
chr8:93822801-93824413	Rpgrip11
chr11:11656565-11664512	Ikzf1
chr11:100663088-100668697	Stat5b
chr14:26272755-26359791	
chr15:10120038-10184431	Prlr
chr16:92701558-92784852	Runx1
chr16:95614472-95706278	Erg
chr2:26321396-26352976	Notch1
chr2:98502691-98502693	
chr2:117164773-117179489	
chr2:163028649-163099637	
chr5:28496409-28496608	En2
chr6:98974529-99018171	Foxp1
chr9:58431692-58566776	
chr9:89864784-89869039	Rasgrf1

Note: The table has two columns one indication the genomic coordinates of the CIS and the second shows any gene within the CIS.

Table A2. Common Insertion Sites (CIS) resulting from the Lck model of Lymphoma in mice.

Locus	Genes
chr1:13283909-13285197	Ncoa2
chr11:45715454-45717555	Clint1
chr11:51094639-51097156	
chr11:117102602-117104929	9-Sep
chr12:113914333-113916396	
chr14:119360457-119361372	Dnajc3
chr11:11603112-11761529	
chr11:100672169-100715001	
chr13:20286545-20344544	Elmo1
chr15:61815527-61914293	
chr16:11080419-11172597	
chr17:51953094-51993825	
chr19:32857358-32876621	Pten
chr2:26321378-26321567	Notch1
chr4:32361368-32515521	Bach2
chr5:28496383-28594034	
chr5:34169482-34192039	Whsc1
chr5:108156691-108171723	
chr6:99116028-99208018	

Note: The table has two columns one indication the genomic coordinates of the CIS and the second shows any gene within the CIS.

Table A3. Common Insertion Sites (CIS) resulting from the CD4 model of Lymphoma in mice.

Locus	Genes
chr13:52037239-52037272	
chr15:97660441-97660441	Hdac7
chr2:92185537-92185676	Phf21a
chr10:66667178-66678128	Jmjd1c
chr11:100668852-100744229	
chr12:113906157-113937487	
chr12:117530220-117531696	Esyt2
chr14:26242047-26266436	
chr14:32599105-32612971	Ankrd28
chr15:61807662-61816592	
chr17:5257408-5281984	Arid1b
chr17:32336596-32360817	Brd4
chr17:47683518-47730095	Ccnd3
chr17:51966211-51989407	
chr17:74967487-74989453	Birc6
chr17:80839505-80848431	Sos1
chr18:7910054-7925447	Wac
chr2:37557045-37569531	
chr2:72776167-72782502	Sp3
chr2:91709387-91755213	Ambra1
chr3:60344064-60410040	Mbnl1
chr3:89853594-89895348	
chr3:103681864-103712615	Ptpn22
chr4:88923521-88935959	Cdkn2a
chr4:100876516-100935515	Jak1
chr4:136040738-136081775	Luzp1
chr5:28496413-28496493	En2
chr5:34143897-34197790	
chr5:100384165-100401722	

Table A3. Contd

chr5:105963241-105979455	Lrrc8c
chr5:108134001-108166022	
chr6:115556842-115621151	
chr7:28367953-28391539	
chr8:26716621-26746241	Whsc111
chr8:109996124-110025131	Wwp2
chr9:31110185-31142324	

Note: The table has two columns one indication the genomic coordinates of the CIS and the second shows any gene within the CIS.

Table A4. gene centric Common Insertion Sites (gCIS) resulting from the Vav model of Lymphoma in mice.

GENE	P-VALUE	NUM_TUMORS
Notch1	0	20
Erg	0	8
Rasgrp1	0	8
Zmiz1	0	7
Rasgrf1	0	5
En2	0	4
Ikzf1	0	4
Stat5b	0	3
Prlr	3.00E-36	3
Foxp1	3.01E-29	3
Myc	0	2
Akt2	5.45E-67	2
Myo1f	4.41E-54	2
Pik3r5	2.46E-49	2
Sfi1	1.13E-46	2
Flt3	5.79E-40	2
Ahnak	2.89E-39	2
Smpd3	6.31E-38	2
Tbc1d23	4.74E-37	2
Tox2	4.55E-36	2
Nptn	6.37E-31	2
Zmynd11	2.82E-29	2
Sos1	1.13E-26	2
Rpgrip1l	2.45E-24	2
Gng12	2.85E-22	2
Xpo7	3.15E-22	2
Nlk	6.95E-19	2
Pcnx	1.16E-18	2
Odz3	1.35E-06	2

Table A4. Contd

Arhgap6	4.00E-05	2
930007M17Rik	4.02E-05	2

Note: The first column indicates the Gene the second is the P-value of the significance of insertions within that particular gene and finally the third column indicates the number of tumors with integration within that particular gene

Table A5. gene centric Common Insertion Sites (gCIS) resulting from the Lck model of Lymphoma in mice.

GENE	P-VALUE	NUM_TUMORS
Stat5b	0	6
Bach2	1.21E-69	6
Whsc1	0	5
Pten	0	4
Myc	0	3
Notch1	0	3
Stat5a	0	3
Ikzf1	3.51E-64	3
Elmo1	1.18E-13	3
Pard3	1.30E-10	3
Akt1	0	2
D10Bwg1364e	0	2
En2	0	2
Samd4b	2.04E-66	2
Spsb1	6.42E-58	2
Dnajc3a	1.97E-50	2
Orc2l	1.72E-45	2
Sfi1	1.84E-42	2
Clint1	3.05E-38	2
Txndc11	4.84E-37	2
2700078E11Rik	6.21E-35	2
2610024E20Rik	4.19E-32	2
Map3k4	1.72E-31	2
1190002A17Rik	1.73E-30	2
Arhgap17	1.73E-30	2
Whsc1l1	1.24E-29	2
Dyrk1a	9.00E-27	2
Herc3	2.36E-25	2
Satb1	7.42E-24	2

Table A5. Contd

Rasgrf1	1.09E-22	2
Clpb	3.56E-22	2
Jak1	4.22E-22	2
Gng12	2.70E-20	2
Upf2	2.35E-19	2
Ash1l	3.58E-19	2
0910001A06Rik	3.11E-18	2
Pds5b	9.92E-16	2
Tbl1x	1.16E-15	2
Fyn	1.43E-15	2
Prkeh	1.43E-15	2
Trerf1	1.46E-15	2
Mllt10	3.31E-14	2
Map3k5	8.75E-13	2
Birc6	2.00E-12	2
Foxp1	2.13E-12	2
Zcchc7	2.19E-12	2
Pitpnc1	5.36E-12	2
Ncoa2	1.07E-11	2
Col23a1	1.32E-11	2
Ext1	1.14E-09	2
Mllt3	4.13E-09	2
Ghr	9.50E-09	2
Adam12	1.29E-08	2

Note: The first column indicates the Gene the second is the P-value of the significance of insertions within that particular gene and finally the third column indicates the number of tumors with integration within that particular gene

Table A6. gene centric Common Insertion Sites (gCIS) resulting from the CD4 model of Lymphoma in mice.

GENE	P-VALUE	NUM_TUMORS
Myc	0	12
Akt2	0	10
En2	0	10
Gfi1	0	9
Whsc1	0	8
Ccnd3	0	6
Jak1	0	6
Phf21a	7.98E-57	6
D030051N19Rik	1.41E-53	6
Cdkn2a	0	5
Brd4	2.32E-83	5
Akt1	0	4
Stat5b	0	4
Raf1	5.08E-75	4
Sos1	2.87E-47	4
Mbnl1	5.19E-30	4
Ankrd28	1.48E-28	4
Birc6	1.66E-23	4
Stk39	1.02E-19	4
Arid1b	1.80E-16	4
Bach2	9.25E-16	4
Lpp	5.48E-08	4
Sp3	4.12E-45	3
Ptpn22	3.19E-42	3
Ncoa3	4.04E-35	3
Lrrc8c	4.63E-32	3
Wac	7.71E-32	3
Luzp1	1.64E-29	3
Wwp2	5.92E-28	3

Table A6. Contd

Satb1	1.62E-26	3
D12Ertd551e	1.78E-25	3
Ttc3	5.54E-24	3
Nsd1	6.32E-23	3
Adam10	1.01E-21	3
Crebbp	4.15E-20	3
Osbpl8	1.13E-18	3
Tbl1xr1	1.78E-18	3
Prlr	8.92E-17	3
Exoc2	9.61E-16	3
Nipbl	2.08E-13	3
Gfi1b	0	2
Gpx3	0	2
Lck	0	2
Letm2	1.68E-86	2
Upf1	3.43E-68	2
4933434E20Rik	1.09E-59	2
BC005537	2.94E-57	2
Stat5a	6.68E-56	2
Il21r	3.33E-45	2
Hdac7a	5.70E-43	2
Rbpms2	1.85E-39	2
Ppp1r2	5.93E-34	2
Rnf170	7.44E-34	2
Hnrpd	3.50E-33	2
Pacsin1	8.36E-32	2
Slc26a8	2.94E-31	2
Son	5.15E-30	2
BC037393	5.46E-29	2
Mtfr1	2.32E-28	2
Ahcy11	3.17E-28	2

Table A6. Contd

Ddx6	3.96E-28	2
Fnbp4	2.95E-27	2
Ppm1a	5.04E-27	2
Gse1	2.77E-25	2
Inpp5b	1.80E-24	2
Zfp592	1.19E-23	2
Pik3r5	5.11E-23	2
Zcchc6	8.61E-23	2
Kif5b	2.00E-22	2
Rassf3	3.76E-22	2
Paqr5	5.55E-22	2
Vrk1	8.63E-20	2
Sh3pxd2b	1.03E-19	2
Ugp2	2.15E-19	2
Prdm10	3.68E-19	2
Nup153	5.16E-19	2
Ncoa6	9.79E-19	2
Ubap2l	2.25E-18	2
Rai1	5.83E-18	2
Pdpk1	7.38E-18	2
Nfatc1	9.88E-18	2
Wasl	1.39E-17	2
Ryk	2.43E-17	2
BC037112	8.26E-17	2
Narg1	3.95E-16	2
Fip1l1	5.91E-16	2
Spred1	6.16E-16	2
Jak2	1.19E-15	2
Nfyc	3.10E-15	2
Setd2	8.36E-15	2
Uimc1	9.13E-15	2

Table A6. Contd

Fkbp5	9.24E-15	2
Traf3	1.71E-14	2
Rbm26	2.65E-14	2
Epc1	3.55E-14	2
Bcar3	6.74E-14	2
Eya3	9.25E-14	2
Eif3h	1.12E-13	2
Rreb1	3.45E-13	2
Fbxl11	3.73E-13	2
Pctk2	5.36E-13	2
Col13a1	5.43E-13	2
Nfkb1	1.25E-12	2
Vav2	2.55E-12	2
Pum2	3.06E-12	2
Hook3	3.47E-12	2
2600010E01Rik	4.55E-12	2
Rasgrf1	9.15E-12	2
Cox10	1.68E-11	2
Mem1	1.83E-11	2
Prr8	3.96E-11	2
Spnb2	1.98E-10	2
Zmiz1	2.29E-10	2
Pi4ka	2.35E-10	2
Cnot2	2.43E-10	2
Galnt7	2.73E-10	2
Eftud1	8.52E-10	2
Ate1	4.21E-09	2
Cbara1	5.54E-09	2
Nlk	5.60E-09	2
Scmh1	6.85E-09	2
Eml4	6.93E-09	2

Table A6. Contd

Epb4.1	7.43E-09	2
Wnk1	1.33E-08	2
A130090K04Rik	1.36E-08	2
Strbp	1.58E-08	2
Rftn1	1.62E-08	2
Ppp2r5e	2.45E-08	2
Arhgap18	2.91E-08	2
Tbl1x	3.48E-08	2
Egfr	3.74E-08	2
Fyn	3.87E-08	2
Utx	8.91E-08	2
Mef2a	1.14E-07	2
Ankrd17	2.01E-07	2
Tle4	2.23E-07	2
1700025G04Rik	2.72E-07	2
Hivep2	4.46E-07	2
Jarid2	6.46E-07	2
Zfand3	9.44E-07	2
Map3k5	1.03E-06	2
Cdyl	1.41E-06	2

Note: The first column indicates the Gene the second is the P-value of the significance of insertions within that particular gene and finally the third column indicates the number of tumors with integration within that particular gene

Table A7. The table below illustrates the gene pair and the p-value of the significance of the interaction for the Vav model of lymphoma in mice

Gene Pair	P-Value
Smpd3-Nlk	0.001587302
Myc-Pcnx	0.001587302
Foxp1-Ahnak	0.004761905

Table A8. The table below illustrates the gene pair and the p-value of the significance of the interaction for the Lck model of lymphoma in mice

Gene Pair	P-Value
Foxp1-Gfi1	0.001221001
Ash1-Ext1	0.002645503
Sfi1-Tbl1x	0.002645503
Gng12-1190002A17Rik	0.002645503
Birc6-Jak1	0.002645503
Birc6-Spsb1	0.002645503
Jak1-Spsb1	0.002645503
Ghr-Pten	0.004737485

Table A9. The table below illustrates the gene pair and the p-value of the significance of the interaction for the CD4 model of lymphoma in mice

Gene Pair	P-Value
Ddx6-Prr8	0.000886525
Rai1-Map3k5	0.000886525
Hnrpd-Ttc3	0.002659574
Ncoa3-A130090K04Rik	0.002659574

Table A10. Common Insertion Sites (CIS) resulting from the Colorectal cancer dataset (Starr et al).

Locus	Gene
chr10:27754043-27961056	Ptprk
chr10:107581818-107796983	Pawr, Ppp1r12a
chr11:3034435-3091599	Sfi1
chr11:86472785-86618762	Cltc, Dhx40, Pthr2
chr12:16856748-16994458	Rock2
chr12:53545183-53660649	Arhgap5
chr12:83296372-83512790	Sipa11
chr13:32253943-32428762	Gmcs
chr13:37950816-38025994	Rreb1
chr13:55328902-55422384	Nsd1, Rab24
chr13:99507105-99714277	Fcho2, Tnpol
chr13:102458227-102543614	Pik3r1
chr13:112221644-112277879	Gpbp1
chr14:79912079-79998101	Elf1, Sugt1
chr14:122485525-122593351	A330035P11Rik, Clybl, Tm9sf2
chr15:42871883-43094231	Eif3e
chr16:38076150-38231623	Gsk3b
chr16:96216709-96345221	Brwd1, Hmgn1
chr17:29090379-29206838	Kctd20, Sfrs3, Stk38
chr17:74935046-75065052	Birc6
chr18:7874331-7972740	Wac
chr18:34271958-34571672	Apc, Pkd2l2, Reep5, Srp19
chr18:35629270-35825208	2010001M09Rik, 5133400G04Rik, Matr3, Paip2, Sil1, Slc23a1, Snora74a
chr18:50050865-50110350	Dmxl1
chr18:73820770-73946223	Elac1, Me2
chr19:32194482-32324193	Sgms1
chr2:20822454-20905542	Arhgap21
chr2:38609630-38728576	Mir181a-2, Mir181b-2, Nr6a1
chr2:90783716-90927503	Cugbp1, Psmc3, Rapsn, Slc39a13

Table A10. Contd

chr2:98495980-98507407	
chr2:143690480-143821932	Dstn, Rrbp1
chr2:152059319-152121433	Tbc1d20
chr3:60338885-60427050	Mbnl1
chr3:84659861-84718415	
chr3:100406662-100517718	
chr4:34942903-35066501	Mobkl2b
chr4:44773413-44932076	Zcchc7
chr4:130226607-130314151	Pum1, Snord85
chr6:18100704-18259550	Cftr
chr6:29427470-29551480	Irf5, Kcp, Tnpo3
chr6:31354970-31422905	Mkln1
chr6:124999055-125101107	Acrbp, Chd4, Iffo1, Lpar5, Nop2
chr7:37314760-37379990	
chr7:150318462-150590532	Kcnq1, Kcnq1ot1
chr8:23948198-24067065	Myst3
chr8:125421642-125612161	Spg7
chr9:71750763-71926347	Tcf12
chr10:128244889-128306030	Ormdl2, Sarnp
chr14:35229557-35309051	Bmpr1a
chr16:13314765-13366425	Mkl2
chr16:90960068-91043789	1810007M14Rik, 4930404I05Rik
chr18:44718616-44795398	Mcc
chr18:64697316-64753894	Atp8b1
chr18:70678854-70758286	Mbd2
chr3:132816038-132906250	9130221D24Rik
chr4:8473072-8531804	Rab2a
chr4:41152280-41219590	Ubap2
chr7:97303257-97362608	Picalm
chr7:108252067-108336010	Fchsd2
chr10:94980431-95004855	Ube2n

Table A10. Contd

chr12:85511413-85559027	C130039O16Rik
chr12:113067677-113103959	Ppp1r13b
chr13:95562479-95603515	Tbca
chr14:98238561-98271393	Dach1
chr5:147054052-147104435	Cdk8
chr6:28521726-28574191	Snd1
chr8:4273103-4315776	Elavl1, Timm44
chr18:34762777-34782440	Brd8
chr2:121863618-121884143	Eif3j, Spg11
chr10:115930162-115935919	Cnot2
chr15:96122423-96132009	
chr3:29908133-29915041	Mecom
chr4:32429626-32429626	Bach2
chr5:99436726-99442501	Prkg2
chr9:59727162-59737526	Myo9a
chr14:71455022-71455022	
chr16:95611851-95612545	Erg
chr18:66678376-66679326	
chr4:43240000-43240000	Unc13b
chr4:73380842-73382240	Rasef
chr5:34928558-34928997	Add1
chr6:103599140-103599204	Chl1
chr9:14125938-14127333	Sesn3
chr9:121505886-121505886	Lyzl4

Note: The table has two columns one indication the genomic coordinates of the CIS and the second shows any gene within the CIS.

Table A11. gene centric Common Insertion Sites (gCIS) resulting from the Colorectal cancer dataset(Starr et al).

GENE	P-VALUE	NUM_TUMORS
Apc	0	36
Wac	7.49E-52	12
Sfi1	1.67E-44	9
Rspo2	1.19E-41	16
Cugbp1	4.18E-35	10
Kcnq1	2.09E-30	17
Ube2n	3.50E-29	6
Cldn15	5.69E-27	3
Brd8	3.35E-24	5
Csnk2a1	1.45E-23	7
Tm9sf2	3.27E-23	7
Gpbp1	2.16E-22	8
Rab24	1.88E-20	2
B430203M17Rik	3.02E-20	3
Rreb1	3.53E-20	8
Tssk2	9.46E-20	2
Nol1	2.23E-19	3
Tcf12	8.89E-19	15
Cltc	1.87E-18	7
Kif20a	5.60E-18	3
Reep6	1.04E-17	2
Pik3r1	1.34E-17	7
Kif1c	1.64E-17	4
Ubap2	1.65E-17	7
Matr3	1.70E-17	5
Notch1	3.17E-17	4
Elavl1	4.18E-17	5
Rab2	4.71E-17	7
Ankrd11	9.27E-17	9
Kctd20	9.36E-17	3
Zcchc7	1.10E-16	11

Table A11. Contd

Ihpk2	1.25E-16	3
Surf2	1.32E-16	2
Tbca	1.48E-16	6
Tssk1	1.51E-16	2
Preli1	2.26E-16	2
Sipa111	2.49E-16	10
Gsk3b	4.41E-16	10
Nip7	6.71E-16	2
Tigd3	6.71E-16	2
Rspo1	7.09E-16	3
Tnp01	9.31E-16	7
Trip6	1.10E-15	2
Ndufv2	1.26E-15	4
Pcsk4	2.23E-15	2
Ldhd	2.65E-15	2
Myst3	2.67E-15	7
Rasl1a	3.73E-15	2
Sar1a	4.26E-15	3
Med22	5.81E-15	2
Timm8b	6.84E-15	2
Cdk8	9.03E-15	6
Dstn	1.05E-14	4
4833436C18Rik	1.59E-14	2
Wdr6	1.96E-14	2
Ppp1r13b	2.07E-14	6
Clps	3.23E-14	2
Arhgap21	6.60E-14	7
2310065K24Rik	1.06E-13	3
Eif3j	1.29E-13	4
Mkln1	1.39E-13	8
Stag3	1.39E-13	4
Trim25	1.49E-13	3
Orai3	1.51E-13	2

Table A11. Contd

Elf1	1.66E-13	7
1700001O22Rik	1.73E-13	2
Tceb2	1.73E-13	2
Tnpo3	1.82E-13	6
Bmpr1a	1.84E-13	7
Suv420h2	1.89E-13	2
Arhgap5	2.50E-13	6
Dctn4	2.81E-13	4
Cish	4.08E-13	2
Cbx2	4.25E-13	2
Gtf2h4	4.43E-13	2
Foxd4	4.81E-13	2
Ugcg	1.07E-12	4
Trib1	1.16E-12	2
Wasf2	1.17E-12	5
Rab5b	1.20E-12	3
Arf3	1.31E-12	3
Slc9a1	1.35E-12	4
Metap2	1.77E-12	4
Mobkl2b	1.85E-12	9
Gpr175	2.55E-12	2
Polr2c	2.55E-12	2
Sesn3	2.62E-12	5
Sipa1	2.65E-12	2
Pum1	2.67E-12	7
Taf9	3.28E-12	3
1700040I03Rik	3.53E-12	2
Rock2	4.91E-12	7
Nr6a1	6.22E-12	10
Ghrl	6.61E-12	2
Tesk1	6.61E-12	2
4930570C03Rik	7.07E-12	2
Ccdc47	9.25E-12	3

Table A11. Contd

1110005A23Rik	1.05E-11	5
Cnot2	1.12E-11	7
Cdkn1b	1.13E-11	2
Tkt	1.30E-11	3
Atp8b1	1.48E-11	7
Otoa	1.48E-11	5
Mbnl1	1.49E-11	8
Sp6	1.56E-11	2
Gmds	1.71E-11	17
B4galt1	2.39E-11	4
8030462N17Rik	2.83E-11	6
Med1	2.83E-11	4
Ralgds	3.38E-11	3
Olfr1263	3.91E-11	2
Supt16h	4.54E-11	4
Grin2d	5.09E-11	3
BC018242	5.23E-11	2
Lass6	9.50E-11	10
Dlg1	9.60E-11	10
Ddb1	1.03E-10	3
Rragc	1.12E-10	3
Ormdl2	1.38E-10	2
Stt3b	1.57E-10	5
Plcb3	1.62E-10	2
Olfr390	2.04E-10	2
Hsd17b12	2.36E-10	7
Gpr21	2.38E-10	2
Olfr389	2.64E-10	2
Cyp1b1	3.46E-10	2
Lmtk2	3.77E-10	5
Spg7	3.82E-10	3
Atp5j2	3.91E-10	2
Narg1	4.88E-10	5

Table A11. Contd

Nckipsd	6.90E-10	2
Pml	7.09E-10	3
Gga1	7.40E-10	2
Picalm	7.69E-10	6
Ipo7	7.72E-10	4
Cst9	7.92E-10	2
Hpcal4	8.29E-10	2
Ephb2	8.32E-10	6
Abcf1	8.67E-10	2
Rhbdd3	9.49E-10	2
Atp2a2	1.03E-09	4
Ppa1	1.05E-09	3
Surf6	1.06E-09	2
2900010J23Rik	1.08E-09	2
A930037G23Rik	1.11E-09	2
Csad	1.38E-09	2
Cep57	1.54E-09	3
Cog8	1.60E-09	2
Chchd3	1.74E-09	10
Mrpl32	1.74E-09	2
AA673488	1.76E-09	3
Gpc2	2.11E-09	2
Hmox2	2.47E-09	3
6332401O19Rik	2.59E-09	2
Nfkbil1	3.04E-09	2
Polr2d	3.10E-09	2
Prdm16	3.40E-09	8
Nsd1	5.13E-09	6
Slc27a5	5.24E-09	2
Arid1b	5.42E-09	10
Rbm35a	5.62E-09	4
Ttc9	5.62E-09	3
2610205E22Rik	5.87E-09	2

Table A11. Contd

Il20rb	6.44E-09	3
Fbn2	6.71E-09	8
Zfp90	7.74E-09	2
9130221D24Rik	7.76E-09	5
Svil	8.02E-09	6
Birc6	1.03E-08	8
Sec63	1.08E-08	5
Med21	1.15E-08	2
Zfp191	1.17E-08	2
Acrbp	1.27E-08	2
Sgms1	1.36E-08	6
Mgat3	1.39E-08	3
Sdhd	1.41E-08	2
1810037C20Rik	1.43E-08	2
Rere	1.53E-08	10
Rcc2	1.67E-08	2
Actr2	1.68E-08	4
Mum1	1.73E-08	2
BC017647	1.89E-08	4
Usp6nl	1.95E-08	6
Myt1	2.02E-08	4
Fchsd2	2.30E-08	8
Brd7	2.36E-08	3
Znrf3	2.44E-08	7
Dhdh	2.64E-08	2
Irf8	2.64E-08	2
Wdr4	2.86E-08	2
Itgb1	3.12E-08	4
Inadl	3.54E-08	10
Sfrs3	3.67E-08	2
Wdr21	3.96E-08	2
Slc19a1	4.48E-08	2
Sltm	4.60E-08	4

Table A11. Contd

Eif2s1	5.23E-08	3
Aldh18a1	5.75E-08	3
Blnk	5.94E-08	4
Ppm2c	6.10E-08	2
Tbc1d13	6.19E-08	2
Fkbp7	7.25E-08	2
Lrrc8d	7.38E-08	5
Psd3	7.93E-08	10
Fhod1	8.12E-08	2
Arid1a	8.32E-08	4
Atxn2	8.76E-08	5
Ptcd3	9.14E-08	3
Prss23	9.34E-08	2
Ddi2	9.79E-08	3
Diap1	1.01E-07	5
Erlin2	1.28E-07	2
Ogdh	1.44E-07	4
Lrrc8b	1.46E-07	4
Dmx11	1.57E-07	7
Tox3	1.58E-07	5
Rbm22	1.62E-07	2
Leng4	1.64E-07	2
Ap1m2	1.72E-07	2
Cxcl15	1.72E-07	2
Atg12	1.79E-07	2
Pcbp2	1.79E-07	3
AW554918	1.83E-07	6
Dsc2	1.94E-07	3
2700078E11Rik	2.03E-07	4
Bop1	2.16E-07	2
1700021C14Rik	2.22E-07	2
Pum2	2.25E-07	5
Spsb1	2.26E-07	3

Table A11. Contd

Usp15	2.29E-07	5
Pard3	2.31E-07	13
Slc6a3	2.43E-07	3
Slc12a9	2.57E-07	2
Ttrap	2.57E-07	2
Man1a2	2.64E-07	6
Cyb5b	2.74E-07	3
Cd2ap	2.81E-07	5
Erg	2.82E-07	6
Btla	2.98E-07	3
Ptprk	3.01E-07	14
Ppp1r12a	3.06E-07	6
Kdelr2	3.08E-07	2
Gprc5a	3.16E-07	2
2310002J15Rik	3.32E-07	1
Aftph	3.40E-07	4
Oxsr1	3.50E-07	4
Fubp1	3.52E-07	3
Golga2	3.72E-07	2
Dio3	3.76E-07	1
Smad4	4.04E-07	4
Ddx55	4.08E-07	2
4933406E20Rik	4.13E-07	2
Cct7	4.13E-07	2
Smcr7l	4.13E-07	2
Farp1	4.17E-07	7
Txn1	4.18E-07	2
Coq9	4.42E-07	2
Rbbp6	4.58E-07	2
1810027O10Rik	4.79E-07	1
Auh	4.84E-07	4
Itga2	4.90E-07	5
Tfg	5.07E-07	3

Table A11. Contd

Centb2	5.28E-07	5
Wnk1	6.29E-07	6
Ubr2	6.34E-07	4
Ndufab1	6.59E-07	2
B3gnt4	7.31E-07	1
Lims1	7.63E-07	5
Memo1	7.63E-07	5
2310011J03Rik	8.16E-07	1
Cdc42	8.75E-07	3
Hip2	8.88E-07	4
Sstr2	9.11E-07	1
Ppp1r16a	9.15E-07	2
Coil	9.25E-07	2
Acly	9.66E-07	3
A730036I17Rik	1.00E-06	2
Dio2	1.01E-06	2
Edc3	1.02E-06	3
Slc9a5	1.02E-06	2
Polk	1.03E-06	4
Pisd	1.07E-06	3
Ankmy2	1.08E-06	3
Fndc3b	1.08E-06	8
Tmprss6	1.08E-06	2
Ppp2r5e	1.14E-06	6
Stau1	1.15E-06	3
Tdrd3	1.25E-06	6
Eif4g1	1.26E-06	2
0610010O12Rik	1.31E-06	3
Them2	1.34E-06	2
BC048651	1.40E-06	2
Fcho2	1.41E-06	5
Ptch1	1.41E-06	3
H1fx	1.43E-06	1

Table A11. Contd

BC051227	1.48E-06	1
Pdxk	1.48E-06	2
Eif3eip	1.51E-06	2
6330569M22Rik	1.52E-06	2
Eif4ebp2	1.52E-06	2
Setd1a	1.52E-06	2
Chuk	1.57E-06	3
Dgcr2	1.67E-06	3
4833409A17Rik	1.69E-06	2
Gm757	1.69E-06	1
Rfc1	1.70E-06	4
Tsc22d2	1.84E-06	4
Pspn	1.87E-06	1
Smarcc1	1.91E-06	5
Ndufs4	1.96E-06	5
Pdxdc1	2.00E-06	4
Stx7	2.01E-06	3
Mbp	2.21E-06	4
Lyzl4	2.22E-06	3
Zfp207	2.24E-06	2
Rad17	2.29E-06	3
Vcl	2.30E-06	5
Phf12	2.31E-06	3
Bace2	2.32E-06	4
Itpkc	2.45E-06	2
Rfxdc2	2.45E-06	5
1110020G09Rik	2.52E-06	3
Snd1	2.59E-06	10
Rnf145	2.62E-06	3

Note: The first column indicates the Gene the second is the P-value of the significance of insertions within that particular gene and finally the third column indicates the number of tumors with integration within that particular gene.

Table A12. Common Insertion Sites (CIS) resulting from the Liver tumor dataset The table has two columns one indication the genomic coordinates of the CIS and the second shows any gene within the CIS.

Locus	Gene
chr4:43405247-43405438	Rusc2
chr12:110838022-110848589	
chr19:3461083-3574380	Saps3
chr5:28496413-28496604	En2
chr8:70492568-70640778	

Note: The table has two columns one indication the genomic coordinates of the CIS and the second shows any gene within the CIS.

Table A13. gene centric Common Insertion Sites (gCIS) resulting from the Liver tumor dataset.

GENE	P-VALUE	NUM_TUMORS
En2	0	6
Saps3	1.77E-69	3
Rusc2	1.80E-88	2
Ptk2b	3.49E-34	2
Rasa2	4.51E-33	2
Zmiz1	1.50E-29	2
Iqgap2	1.25E-15	2
Pip5k1b	2.00E-15	2
Pde3a	4.94E-14	2
Faf1	1.26E-10	2
Stag1	9.20E-10	2
Dip2c	2.97E-09	2
Rabgap11	2.39E-06	2

Note: The first column indicates the Gene the second is the P-value of the significance of insertions within that particular gene and finally the third column indicates the number of tumors with integration within that particular gene.

Table A14. Common Insertion Sites (CIS) resulting from the Skin cancer dataset.

Locus	Gene
chr19:32838991-32854236	Pten
chr4:77035987-77082221	
chrX:142107713-142135531	
chr14:26463292-26463869	Zmiz1
chr5:28496409-28496604	En2

Note: The table has two columns one indication the genomic coordinates of the CIS and the second shows any gene within the CIS.

Table A15. gene centric Common Insertion Sites (gCIS) resulting from the Skin cancer dataset.

GENE	P-VALUE	NUM_TUMORS
Zmiz1	0	14
En2	0	4
Pten	0	2

Note: The first column indicates the Gene the second is the P-value of the significance of insertions within that particular gene and finally the third column indicates the number of tumors with integration within that particular gene

REFERENCES

- Amsterdam, A., Burgess, S., Golling, G., Chen, W., Sun, Z., Townsend, K., Farrington, S., Haldi, M., & Hopkins, N. (1999). A large-scale insertional mutagenesis screen in zebrafish. *Genes & Development*, *13*(20), 2713.
- Cappuzzo, F., Hirsch, F. R., Rossi, E., Bartolini, S., Ceresoli, G. L., Bemis, L., Haney, J., Witte, S., Danenberg, K., & Domenichini, I. (2005). Epidermal growth factor receptor gene and protein and gefitinib sensitivity in non-small-cell lung cancer. *JNCI Journal of the National Cancer Institute*, *97*(9), 643.
- Collier, L. S., Carlson, C. M., Ravimohan, S., Dupuy, A. J., & Largaespada, D. A. (2005). Cancer gene discovery in solid tumours using transposon-based somatic mutagenesis in the mouse. *Nature*, *436*(7048), 272-276.
- Davidson, A. E., Balciunas, D., Mohn, D., Shaffer, J., Hermanson, S., Sivasubbu, S., Cliff, M. P., Hackett, P. B., & Ekker, S. C. (2003). Efficient gene delivery and gene expression in zebrafish using the Sleeping Beauty transposon. *Developmental Biology*, *263*(2), 191-202.
- De Ridder, J., Uren, A., Kool, J., Reinders, M., & Wessels, L. (2006). Detecting statistically significant common insertion sites in retroviral insertional mutagenesis screens. *PLoS Comput Biol*, *2*(12), e166.
- Dupuy, A. J., Akagi, K., Largaespada, D. A., Copeland, N. G., & Jenkins, N. A. (2005). Mammalian mutagenesis using a highly mobile somatic Sleeping Beauty transposon system. *Nature*, *436*, 221-226.
- Dupuy, A. J., Jenkins, N. A., & Copeland, N. G. (2006). Sleeping beauty: a novel cancer gene discovery tool. *Human Molecular Genetics*, *15*, R75.
- Easton, D. F., Pooley, K. A., Dunning, A. M., Pharoah, P. D. P., Thompson, D., Ballinger, D. G., Struwing, J. P., Morrison, J., Field, H., & Luben, R. (2007). Genome wide association study identifies novel breast cancer susceptibility loci. *Nature*, *447*(7148), 1087-1093.
- Ewing, B., & Green, P. (1998). Base-calling of automated sequencer traces using Phred. II. error probabilities. *Genome Research*, *8*(3), 186.
- Gavin, A., Scheetz, T., Roberts, C., O'Leary, B., Braun, T., Sheffield, V., Soares, M., Robinson, J., & Casavant, T. (2002). Pooled library tissue tags for EST-based gene discovery. *Bioinformatics*, *18*(9), 1162.

- Gordon, D. (2003). Viewing and editing assembled sequences using Consed. *Current Protocols in Bioinformatics / Editorial Board, Andreas D.Baxevanis ...[Et Al.]*, Chapter 11, Unit11.2. doi:10.1002/0471250953.bi1102s02
- Griffiths, A. J. F., Miller, J. H., Suzuki, D. T., Lewontin, R. C., & Gelbart, W. M. (2000). *An introduction to genetic analysis* WH Freeman New York:.
- Hanahan, D., & Weinberg, R. A. (2000). The hallmarks of cancer. *Cell*, 100(1), 57-70.
- He, L., Thomson, J. M., Hemann, M. T., Hernando-Monge, E., Mu, D., Goodson, S., Powers, S., Cordon-Cardo, C., Lowe, S. W., & Hannon, G. J. (2005). A microRNA polycistron as a potential human oncogene. *Nature*, 435(7043), 828-833.
- Hillier, L. D. W., Marth, G. T., Quinlan, A. R., Dooling, D., Fewell, G., Barnett, D., Fox, P., Glasscock, J. I., Hickenbotham, M., & Huang, W. (2008). Whole-genome sequencing and variant discovery in *C. elegans*. *Nature Methods*, 5(2), 183-188.
- Jonkers, J., Korswagen, H. C., Acton, D., Breuer, M., & Berns, A. (1997). Activation of a novel proto-oncogene, *Frat1*, contributes to progression of mouse T-cell lymphomas. *The EMBO Journal*, 16(3), 441-450.
- Kent, W. J. (2002). BLAT-The BLAST-Like Alignment Tool. *Genome Research*, 12(4), 656-664.
- Kile, B. T., & Hilton, D. J. (2005). The art and design of genetic screens: mouse. *Nature Reviews Genetics*, 6(7), 557-567.
- Kool, J., & Berns, A. (2009). High-throughput insertional mutagenesis screens in mice to identify oncogenic networks. *Nature Reviews Cancer*, 9(6), 389-399.
- Langmead, B., Trapnell, C., Pop, M., & Salzberg, S. (2009). Ultrafast and memory efficient alignment of short DNA sequences to the human genome. *Genome Biology*, 10(3), R25.
- Levenshtein, V. I. *Binary Codes Capable of Correcting Deletions, Insertions*,
- Li, C., Kim, S. W., Rai, D., Bolla, A. R., Adhvaryu, S., Kinney, M. C., Robetorye, R. S., & Aguiar, R. C. T. (2009). Copy number abnormalities, MYC activity, and the genetic fingerprint of normal B cells mechanistically define the microRNA profile of diffuse large B-cell lymphoma. *Blood*, 113(26), 6681.
- Li, H., Ruan, J., & Durbin, R. (2008). Mapping short DNA sequencing reads and calling variants using mapping quality scores. *Genome Research*, 18(11), 1851.
- Lu, B., Geurts, A. M., Poirier, C., Petit, D. C., Harrison, W., Overbeek, P. A., & Bishop, C. E. (2007). Generation of rat mutants using a coat color-tagged Sleeping Beauty transposon system. *Mammalian Genome*, 18(5), 338-346.

- Matros, E., Wang, Z. C., Richardson, A. L., & Iglehart, J. D. (2004). Genomic approaches in cancer biology. *Surgery*, *136*(3), 511-518.
- Meltzer, P. S. (2005). Small RNAs with big impacts. *Nature*, *435*, 9.
- Moressi, C. J. (2007). *Integration analysis system to computationally and functionally characterize integration sites*
- Pedraza-Farina, L. G. (2006). Mechanisms of oncogenic cooperation in cancer initiation and metastasis. *The Yale Journal of Biology and Medicine*, *79*(3-4), 95-103.
- Pruitt, K. D., Tatusova, T., & Maglott, D. R. (2006). NCBI reference sequences (RefSeq): a curated non-redundant sequence database of genomes, transcripts and proteins. *Nucleic Acids Research*,
- Rice, P., Longden, I., & Bleasby, A. (2000). EMBOSS: the European molecular biology open software suite. *Trends in Genetics*, *16*(6), 276-277.
- Russell, W., Kelly, E., Hunsicker, P., Bangham, J., Maddux, S., & Phipps, E. (1979). Specific-locus test shows ethylnitrosourea to be the most potent mutagen in the mouse. *Proceedings of the National Academy of Sciences of the United States of America*, *76*(11), 5818-5819.
- Schulz, W. A. (2007). *Molecular biology of human cancers: an advanced student's textbook* Springer Verlag.
- Shannon, P., Markiel, A., Ozier, O., Baliga, N. S., Wang, J. T., Ramage, D., Amin, N., Schwikowski, B., & Ideker, T. (2003). Cytoscape: a software environment for integrated models of biomolecular interaction networks. *Genome Research*, *13*(11), 2498.
- Slonim, D. K., & Yanai, I. (2009). Getting started in gene expression microarray analysis. *PLoS Computational Biology*, *5*(10)
- Spradling, A. C., Stern, D., Beaton, A., Rehm, E. J., Laverty, T., Mozden, N., Misra, S., & Rubin, G. M. (1999). The Berkeley Drosophila Genome Project Gene Disruption Project Single P-Element Insertions Mutating 25% of Vital Drosophila Genes. *Genetics*, *153*(1), 135-177.
- Starr, T. K., Allaei, R., Silverstein, K. A. T., Staggs, R. A., Sarver, A. L., Bergemann, T. L., Gupta, M., O'Sullivan, M. G., Matise, I., & Dupuy, A. J. (2009). A transposon-based genetic screen in mice identifies genes altered in colorectal cancer. *Science*, *323*(5922), 1747.
- Theodorou, V., Kimm, M. A., Boer, M., Wessels, L., Theelen, W., Jonkers, J., & Hilken, J. (2007). MMTV insertional mutagenesis identifies genes, gene families and pathways involved in mammary cancer. *Nature Genetics*, *39*(6), 759-769.

Weaver, R. F. (1998). *Molecular Biology*, WCB.

Wood, L. D., Parsons, W. D., Jones, S., Lin, J., Sjoblom, T., Barber, T., Parmigiani, G., Velculescu, V., Kinzler, K. W., & Vogelstein, B. (2008). *Genomic Landscapes of Human Breast and Colorectal Cancers*,